

Validation of CAE based Methodology to Predict Sloshing Noise in Automotive Fuel Tank

Kothari Mayur N.

Under the guidance of

Dr. B.Venkatesham



भारतीय प्रौद्योगिकी संस्थान हैदराबाद
Indian Institute of Technology Hyderabad

Department of Mechanical Engineering

September 2015

Declaration

I declare that this written submission represents my ideas in my own words, and where ideas or words of others have been included, I have adequately cited and referenced the original sources. I also declare that I have adhered to all principles of academic honesty and integrity and have not misrepresented or fabricated or falsified any idea/data/fact/source in my submission. I understand that any violation of the above will be a cause for disciplinary action by the Institute and can also evoke penal action from the sources that have thus not been properly cited, or from whom proper permission has not been taken when needed.



(Signature)

(Kothari Mayur N.)

ME13M1010

(Roll No.)

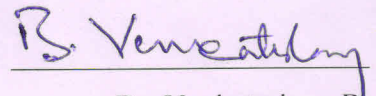
Approval Sheet

This thesis entitled "Validation of CAE based methodology to predict sloshing noise in an Automotive Fuel Tank" by Mayur Kothari is approved for the degree of Master of Technology from IIT Hyderabad.



Dr. Amirtham Rajagopal

Assistant Professor,
Department of Civil Engineering,
Indian Institute of Technology, Hyderabad
Examiner



Dr. Venkatesham B.

Assistant Professor,
Department of Mechanical and Aerospace Engineering,
Indian Institute of Technology, Hyderabad
Adviser



Dr. Raja Banerjee

Associate Professor,
Department of Mechanical and Aerospace Engineering,
Indian Institute of Technology, Hyderabad
Co-Adviser

Acknowledgements

The work presented here would not have been possible without the guidance and support of many people who in one way or the other extended their valuable assistance. I take this opportunity to express my sincere gratitude towards them.

First and foremost, I express my deep gratitude to my guide Dr. B .Venkatesham for offering me a challenging project like this, reposing confidence that this would be executable by me in the given time frame, and providing valuable guidance, professional advice, thoughtful suggestions and mature conduct.

A very special thanks to Dr. Ra ja Banerjee, for his continuous support, suggestions and thoughtful interventions at all stages of this project.

I would like to thank each and every faculty of my department for their guidance throughout my course work. I would like to thank IIT Hyderabad for providing resources in carrying out my research work.

The role and support of family is quintessential. I fall short of words to thank my parents and sister Deepti for all the patience, support and motivation.

I would like to thank Mercedes-Benz Reserch & Developement India, for giving me opportunity to work on real world problem and financial support for my project.

I mention my deep thankfulness to my project colleague Atul for supporting and helping me throughout my project.

I would like to thank workshop in charge Mr.Satyanarayana and workshop personnel Mr.Madhu, Mr.Brahmachari, Mr.Ashok, Mr.Jagadeeshan, Mr.Kiran Kumar, Mr. Praveen and every other workshop personnel without whose help the set up for experiment could not have been completed.

I extend my thanks to all my lab mates Girish, Varun, Tapan, Nagaraj, Sachin, Amogh, Pravin for their support in my work.

I am very much thankful to my dear friends Yogesh, Yagnik, Milind, Pratap, Naresh, Shweta, Deepsikha, Rakesh, Anil for their support and making my stay in IITH one of the most memorable ones.

I am also thankful to each and every member of IIT Hyderabad who had been supportive throughout my stay here for the last two years.

Abstract

Due to advancement in technology major noise sources in an automotive car such as engine, transmission, aerodynamic noise, tyre road noise have significantly reduced. Thus sources of noise such as sloshing noise in a fuel tank which previously did not contribute much in the overall SPL have become more significant now. Also in high end luxury cars and hybrid cars sloshing noise is considered as an irritant. All major international OEMs and their suppliers try to reduce sloshing noise by various design modifications in the fuel tank. However, most major activities reported in open literature are primarily based on performing various CAE and experimental studies in isolation. At the same time, noise generation and its propagation is a multiphysics phenomenon, where fluid mechanics due to liquid sloshing affects structural behaviour of the fuel tank and its mountings which in turn affects noise generation and propagation. In the present study, a multiphysics approach to noise generation has been used to predict liquid sloshing noise from a rectangular tank. By taking Computational Fluid dynamics (CFD) data, Finite Element Method (FEM) simulation studies have been performed in a weakly coupled manner to predict noise. Effect of fluid fill level on dynamic behavior of tank and generated noise is also incorporated in the numerical methodology. Sloshing noise generated due to fluid interaction with structural walls is simulated using Vibro-acoustic model. An integrated model is developed and validated to predict dynamic forces and vibration displacement on tank walls due to dynamic pressure loading on tank walls. Noise radiated from tank walls is modelled by transient Finite Element method. Experimental and numerical studies have been performed to understand the mechanics of sloshing noise generation. Images from high speed video camera and noise measurement data have been used to compare numerical results. Thus peak SPL and dynamic acceleration of tank walls from experiments and numerical method are compared and comparison is also made in the frequency domain.

Contents

Declaration	ii
Approval Sheet	iii
Acknowledgements	iv
Abstract	v
Nomenclature	vii
1 Introduction	1
1.1 Definition	1
1.1.1 Motivation	2
1.2 Literature Survey	3
2 Theoretical Background	5
2.1 Modal analysis	5
2.2 Transient dynamic analysis	6
2.3 Acoustic simulation	7
2.3.1 Acoustic Boundary Element Method Vs. Acoustic Finite Element Method	7
2.3.2 Selection of time-step	8
2.4 Selection of field points	8
2.5 Coupling methods	10
3 Experimental Setup	13
3.1 Subsystem details	15
4 Numerical Analysis	19
4.1 Fluid Structure Interaction (FSI) coupling	19
4.2 Co-Simulation Methodology	19
4.3 Sloshing Noise Prediction Methodology	20
4.4 Structural Simulation	22

5	Results and discussion	25
5.1	Experimental Analysis	25
5.1.1	Parametric Study	25
5.1.2	Sloshing Natural Frequency Estimation - Analytical, Experimental and Numerical	26
5.1.3	Modal Analysis	29
5.1.4	Experimental Results	32
5.1.5	Consolidated Experimental Results	42
5.1.6	Numerical Results	46
5.1.7	Comparison between Experimental and Numerical SPL	52
6	Summary and Future Scope	54
6.1	Summary	54
6.2	Future Scope	54

Chapter 1

Introduction

1.1 Definition

Liquid fuel in a partially filled automotive tank oscillates when subjected to sudden acceleration or deceleration. This low frequency oscillation of free surface is called liquid sloshing and is one of the source of noise generation in an automobile. Due to sloshing, complex surface waves are generated and dynamic forces are exerted on the tank walls. This results in noise generation which is typically referred as sloshing noise.

Figure. 1.1 shows the classification of sloshing noise and its generation mechanism

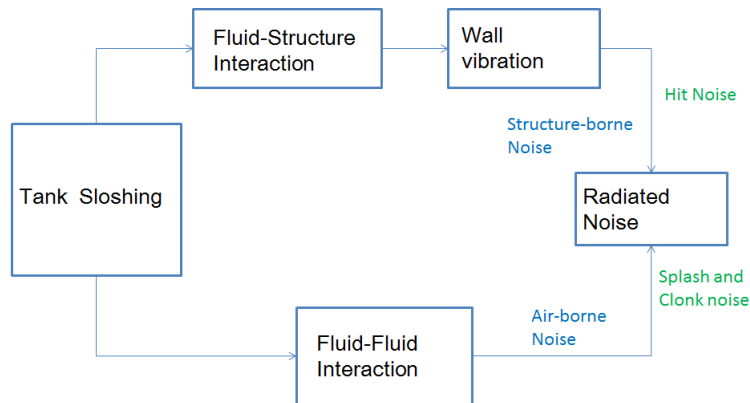


Figure 1.1: Sloshing noise classification

1. Hitting noise - noise radiation due to tank wall vibration

Under sudden acceleration or deceleration fluid in the tank moves and hits the tank walls causing wall vibrations and subsequently noise generation. This is known as fluid-structure interaction. The vibration that occurs in the tank is mainly transferred as structure-borne vibration that is heard as hitting noise at the observation location and it occurs generally at lower frequencies in the range of 50 Hz to 500 Hz.

2. Splashing noise - noise resulting from fluid-fluid interaction

Also under external excitation forces, the free surface waves interact with each other i.e. there is fluid-fluid interaction, which creates pressure pulses inside the fuel tank. It is mainly transmitted as air-borne noise that transmits exterior through tank walls. The noise due to fluid-fluid interaction is known as splashing noise which generally occurs at higher frequencies in the range of 500 Hz to 10 kHz.

3. Clonk noise - noise resulting from fluid-air interaction

This type of noise is generated when abrupt compression of air by sloshing liquid takes place. It's intensity as well as application time is lowest among the three and it occurs in the frequency range of 150-500 Hz.

1.1.1 Motivation

Due to dramatic minimization of other sources of noise generation in an automobile like exhaust, power train, tyre and air-borne noise, noise generation due to sloshing in the fuel tank is getting increased attention as it is considered to be an irritant for the passenger in the vehicle.

The sloshing noise which passengers can hear is produced in a quiet driving condition such as parking their cars in a quiet parking lot. Sloshing is a complicated problem and generally treated numerically as fluid structure interaction problem. Sloshing has plenty of application in automotive, marine transportation and aerospace industry.

Also previous work was carried out on Impact Test Setup (ITS) rig which simulated the actual acceleration and deceleration and thus actual forcing condition on the fuel tank. Here the three regions of sloshing i.e. non linear, transition and linear were observed in one single run of the experiment.[?]

To have finer control on external excitation and observe the three regions of sloshing separately, the present study included development of a Reciprocating Test Setup (RTS) so that behaviour of sloshing fluids under controlled conditions could be studied.

Many factors influence slosh noise performance, including:

1. Fuel Tank material properties like elasticity, density and stiffness,
2. Fuel type and fill level,
3. Vehicle acceleration and deceleration level,
4. Geometry and shape of the tank shell (eg.baffles,pads etc.),
5. Other objects inside the tank(eg. feed pump) which are impacted by moving fuel.

Therefore, a simulation to predict slosh noise should include these critical parameters.

1.2 Literature Survey

Varun et al [?] developed a sloshing noise prediction methodology for rectangular tank using CFD, FEM, and acoustic BEM method.

Based on their experimental work, Wachowski et al [?] classified sloshing noise into three categories: Splash, Hit and Clonk noise. Each of these three categories of noise occur at distinct range of frequencies and is found out using wavelet analysis. They concluded optimisation of the tank structure can achieve lower noise emission and vibration.

Kamei et al [?] determined a sloshing noise correlation that relates factors pertaining to the fuel tank, body parts and tank mounting structure. The tank mounting structure which is related to both the fuel tank and the body parts has the largest contribution to sloshing noise. Also he catagorized the low frequency structure borne noise and high frequency air borne noise.

Kamiya et al [?] used coupled analysis to study interaction between fluid and structure models to predict sloshing using MSC.Dytran. They studied effect of baffle configurations and fluid level on sloshing dynamics.

De Man and Van Schaftingen [?] performed a source-path-receiver analysis for both structural and air borne noise for a sloshing fuel tank.

Wiesche [?] derived a correlation between slosh noise pressure fluctuations within the sloshing liquid. He used two-phase Computational Fluid Dynamics (CFD) to track liquid interface within realistic tank geometries to determine these pressure fluctuations. He discussed effect of anti-slosh element (Baffles and pads) on the slosh dynamics. However prediction about the absolute sound level cannot be made.

Park et al [?] used a Fluid Structure Interaction (FSI) approach to predict noise due to sloshing. Also they carried out numerical optimization of parameters to reduce computation time.

Vytla and Ando et al [?] performed a one-way coupled FSI analysis. They studied the effect of deceleration magnitude for different fuel tank fill level.

Khezzer et al. [?] studied sloshing in rectangular tank subjected to impulsive force and concluded that flow visualization of experimental and numerical simulation were similar.

Hattori et al [?] studied different types of waves generated due to sloshing and classified them on the basis of impact pressure pattern achieved during experimentation with a specific type of wave.

Thiagrajan et al. [?] worked on sloshing in a rectangular tank using sway excitation and observed that 20 % and 80 % of fill level, causes higher pressure than other condition.

Hou et al. [?] applied multiple excitations on a rectangular tank and concluded that liquid sloshing become violent and intensified if sloshing tank is under multiple coupled excitations.

Peric and Zorn [?] studied structural impact of sloshing loads caused by arbitrary motion of tank. The numerical simulation shows agreement with the experiment. It is also found

that there is negligible difference between result in turbulence and laminar model.

Jaiswal et al [?] have conducted Experimental and numerical studies on sloshing and have obtained the sloshing frequency of liquid contained in tanks of other shapes and tanks with internal obstructions using Electro-Magnetic Shake Table and ANSYS software.

Hoi Sum IU et al [?] compared mean kinetic energy and average turbulent kinetic energy of the fluid with sound measurements obtained from the slosh experiments on RTS.

Fan Li et al [?] used de-coupled fluid /structure interaction (FSI) to predict sloshing noise.

Thus various experiments have been performed and numerical methodologies have been developed to predict forces due to fluid sloshing, effect of fluid fill on tank dynamics and prediction of sloshing noise. However, a validated multi-physics model to predict sloshing noise and comparison with experimental results is required.

Chapter 2

Theoretical Background

Sloshing noise analysis is a multiphysics problem. So, it is essential to understand different approaches to solve this problem, basic governing equations and principles for different analysis technique like modal analysis, transient dynamic analysis and acoustic analysis.

2.1 Modal analysis

Modal analysis is used to determine the dynamic/vibration characteristic of system. Modal analysis determines the natural frequency, mode shapes and mode participation factor (how much a given mode participates in a given direction). Natural frequency and mode shapes are important parameters in the design of structure for dynamic loading condition like transient loading, harmonic loading etc. Assumptions considered for modal analysis are, structure has constant stiffness and mass effect, no damping, no time varying forces and pressure acting on structure (pressure). For sloshing problem, modal analysis is performed in order to demonstrate the contribution of the structural properties of the tank in the slosh noise prediction. The equation of motion for undamped system expressed in matrix notation [?]

$$[M] \{\ddot{u}\} + [K] \{u\} = \{0\} \quad (2.1)$$

Where,

M - mass matrix;

K - stiffness matrix;

u - displacement

For linear system, free vibration will be harmonic of the form

$$\{u\} = [\phi]_i \sin \omega_i t$$

where,

$[\phi]_i$ = eigenvector representing mode shape of the i^{th} natural frequency

$\omega_i = i^{th}$ circular natural frequency (radians per unit time)

t = time

Thus the equation of motion becomes,

$$(-\omega_i^2[M] + [K])\{\phi_i\} = \{0\}$$

The above condition is satisfied only when determinant of $(-\omega_i^2[M] + [K])$ is zero because the other condition $\{\phi_i\} = \{0\}$ gives trivial solution.

Thus,

$$[-\omega_i^2[M] + [K]] = 0$$

This is eigen value problem may be solved upto n values of natural frequencies and n values of mode shapes where n is number of degrees of freedom.

2.2 Transient dynamic analysis

Transient dynamic analysis is a technique used to determine the dynamic response of structure under the action of any time-dependent loads. Output of this analysis is used to determine time-varying displacement, strain, stress etc. The project work involves the transient dynamic analysis which determines transient response of structure under the action of impulsive load due to liquid sloshing on the walls of the tank. The load which acts on structure for small duration of time with high value of magnitude is characterised as impulsive load. Since an ideal impulse force excites all modes of a structure.

The basic governing equation of motion for multi-degree freedom system is given as [?],

$$[M] \{\ddot{u}\} + [C] \{\dot{u}\} + [K] \{u\} = \{F^a\} \quad (2.2)$$

Where,

$[M]$ = Structural mass matrix

$[C]$ = Structural damping matrix

$[K]$ = Structural stiffness matrix

$\{\ddot{u}\}$ = Nodal acceleration vector

- $\{u\}$ = Nodal velocity vector
- $\{u\}$ = Nodal displacement vector
- $\{F^a\}$ = Applied load vector

2.3 Acoustic simulation

2.3.1 Acoustic Boundary Element Method Vs. Acoustic Finite Element Method

1. Acoustic boundary element method (BEM Acoustic)

Boundary element method reduces complex three dimensional geometry to two-dimensional surface and only discretization of boundary is sufficient in these methods. Basis functions are selected in such way that it should satisfy the governing partial differential equation. Undetermined coefficients are estimated by satisfying the boundary conditions. This method can be used for internal and external sound radiation problems [?].

2. Acoustic finite element method (FEM Acoustic)

In finite element method [?], acoustic volume is discretized. Basis function is selected in such a way that it should satisfy boundary condition exactly. Undetermined coefficients are determined by satisfying governing partial differential equation.

- Governing equation and boundary condition involved in acoustic analysis are

$$\nabla^2 p(\vec{x}, t) = \frac{1}{c^2} \frac{\partial^2 p(\vec{x}, t)}{\partial t^2} \quad (2.3)$$

Where, $\nabla^2 = \frac{\partial^2}{\partial x^2} + \frac{\partial^2}{\partial y^2} + \frac{\partial^2}{\partial z^2}$ for rectangular co-ordinate system

Assuming time is harmonic in nature, acoustic wave equation becomes, Helmholtz Equation

$$\begin{aligned} \nabla^2 \bar{p}(\vec{x}) + k^2 \bar{p}(\vec{x}) &= 0 \\ p &= \text{Re}(\bar{p}(\vec{x}) e^{i\omega t}) \end{aligned}$$

Where, k is wave number and is defined as

$$k = \omega/c$$

Generally, three types of boundary conditions are used which are normal components of surface velocity, surface pressure, acoustic impedance at the surface.

Surface velocity boundary condition is preferred to apply because it is (i) insensitive to surrounding acoustic field (ii) accurate to measure (iii) easy to predict numerically.

The numerical method used for acoustic analysis is a boundary element method that solves Kirchoff-Helmholtz integral equations with normal surface vibration velocity as boundary conditions. Commercial acoustic software LMS Virtual Lab is used in this study.

2.3.2 Selection of time-step

In dynamic analysis, inertia, stiffness, damping and load plays important role, effect of these factors is captured only when accurate timestep is selected in the analysis. If these factors are not important then static analysis is also sufficient. The accuracy of the transient dynamic solution depends on the integration time step. Smaller time step provides higher accuracy. When time step is too large, then there will be error in calculating higher modes response and overall response of structure. In opposite when time step is too small then solving such system is computationally very expensive. Optimum time step size depend on response frequency of structure. Dynamic response of structure is a combination of all modes, so, it is essential to choose time step such that it should be able to resolve the highest mode that contributes to response. Optimum time step can be chosen based on highest frequency [?], f_{max} , as follows,

$$\text{Integration time step} = 1/20f_{max}$$

2.4 Selection of field points

The sound field radiated by a source in a free field may be divided into three regions [?]: Hydrodynamic near field, Geometric (or Fresnel) near field, and Far field as shown in Figure. 2.1.

1. Hydrodynamic near field

The region immediately adjacent to the vibrating surface of the source is considered as the hydrodynamic near field, and this region is dominant upto a distance much less than one wavelength. In this region, the acoustic pressure is out of phase with local particle velocity.

2. Geometric near field

The geometric near field is next to the hydrodynamic near field. In this region, interference between contributing waves from various parts of the source lead to interference effects and sound pressure levels that do not necessarily decrease monotonically at the rate of 6 dB for each doubling of the distance from the source. Acoustic pressure amplitude in the near field may not give the actual sound power radiated by the source.

3. Far field

Acoustic pressure and acoustic particle velocity are in phase in far field. In the far field, sound pressure levels decrease monotonically at the rate of 6 dB for each doubling of the distance from the source and the source directivity is well defined. Measurement of sound pressure level in far field is preferred.

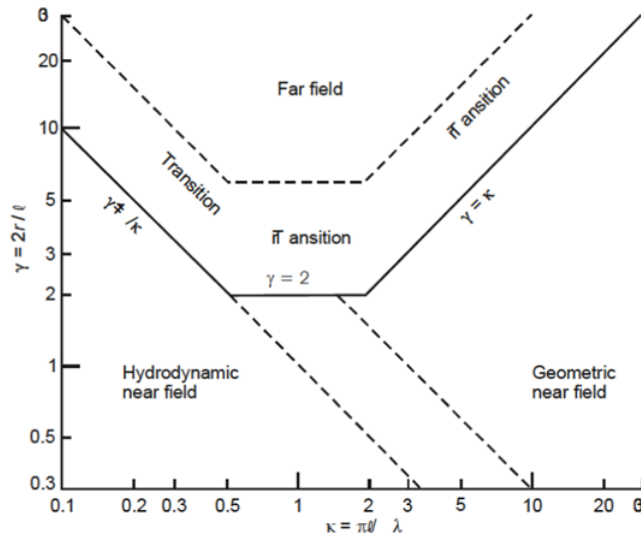


Figure 2.1: Radiation field of source

To characterise the far field, following three equation need to be satisfied,

$$r \gg \lambda/2\pi, \quad r \gg l, \quad r \gg \pi l^2/2\lambda$$

Where,

r is the distance from the source to the measurement position,

λ is wavelength of radiated sound,

l is characteristic source dimension.

More generally defining,

$$\gamma = 2r/l, \quad \kappa = \pi l/\lambda,$$

using these parameters radiation of sound field is classified.

Hitting noise and clonking noise are dominant at 50 Hz to 2000 Hz, so considering this frequency ranges, field point/microphones location is selected in a such way that will satisfy the above three criteria for far field.

2.5 Coupling methods

Coupling equation between fluid and structure can be solved using two approaches [?]

1. Strong Coupling :

In this approach, to find the solution of coupled problem all governing equation (here for fluid, Navier-stokes equation and for structure, equation of motion) are combined in large system and then solved. At the interface fluid solver and FEM solver solve the equation simultaneously. The solution obtained from this approach is stable. But solving a system with strong coupling is often difficult as it is computationally expensive.

2. Weak Coupling :

In this approach, each problem is solved separately and some variables are exchanged and inserted into the equation of other problem. In weak coupling each solver solves the equation until convergence is achieved and then transfers data to other solver. Data can be exchanged in one way or two way coupled approach. This coupling gives less exact solution compared to strong coupling but advantage is that sub-problem can be solved faster than the complete system.

As explained above, exchange of the information between two solvers can take place in two ways one way coupling and two way coupling [?]:

1. One way coupling

Due to fluid motion, pressure load acts on structure. If the reaction of structure on fluid is negligible then this type of coupling is treated as one way coupling. For this type of problem, as control volume of structure is not changing much, it may be sufficient to use only one way mapping of fluid pressure to the structure.

Figure. 2.2 explains the one way coupling method. First, CFD solver solves the fluid flow equation until convergence is achieved and then resulting pressure is mapped/interpolated on structural mesh. Structural solver solves structural dynamic equation upto the convergence. The process repeated until the end time is reached.

2. Two way coupling

Due to fluid motion, pressure load acts on structure. If the control volume of the fluid region changes measurably/significantly then this type of problem needs two way coupling approach. Generally, for flexible structure (for low modulus of elasticity) two way coupling is preferred.

Figure. 2.3 shows the flowchart of two way coupled approach. First, Fluid solver solves the fluid flow equation and generated pressure data is mapped/interpolated on structural

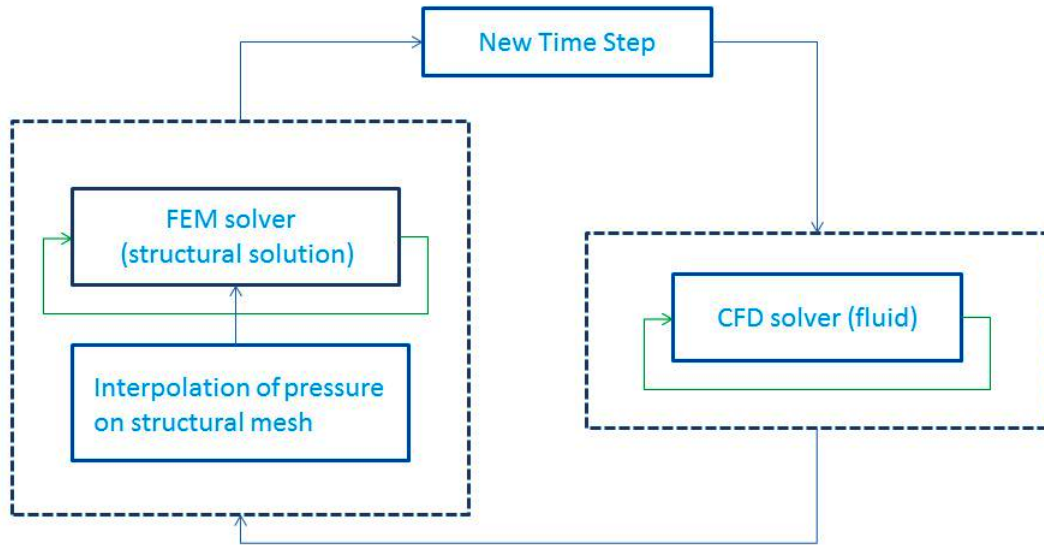


Figure 2.2: Flowchart of one way coupling

mesh. In structural dynamic analysis, CFD pressure data is acts as a boundary condition for structural analysis. Deformation from structural solver is mapped on fluid mesh. Both solver solves the equations until convergence is reached, and then it goes to next time step.

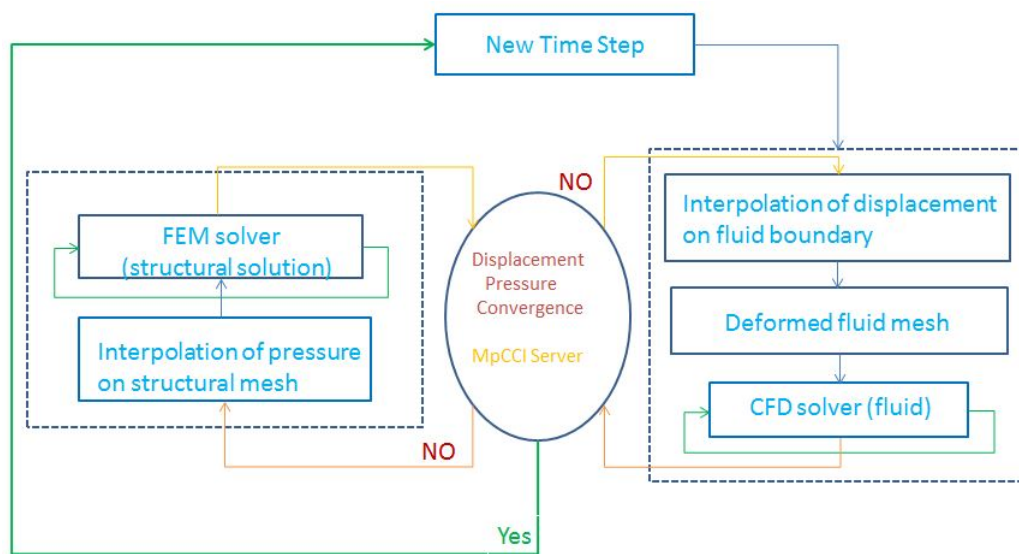


Figure 2.3: Flowchart of two way coupling

Chapter 3

Experimental Setup

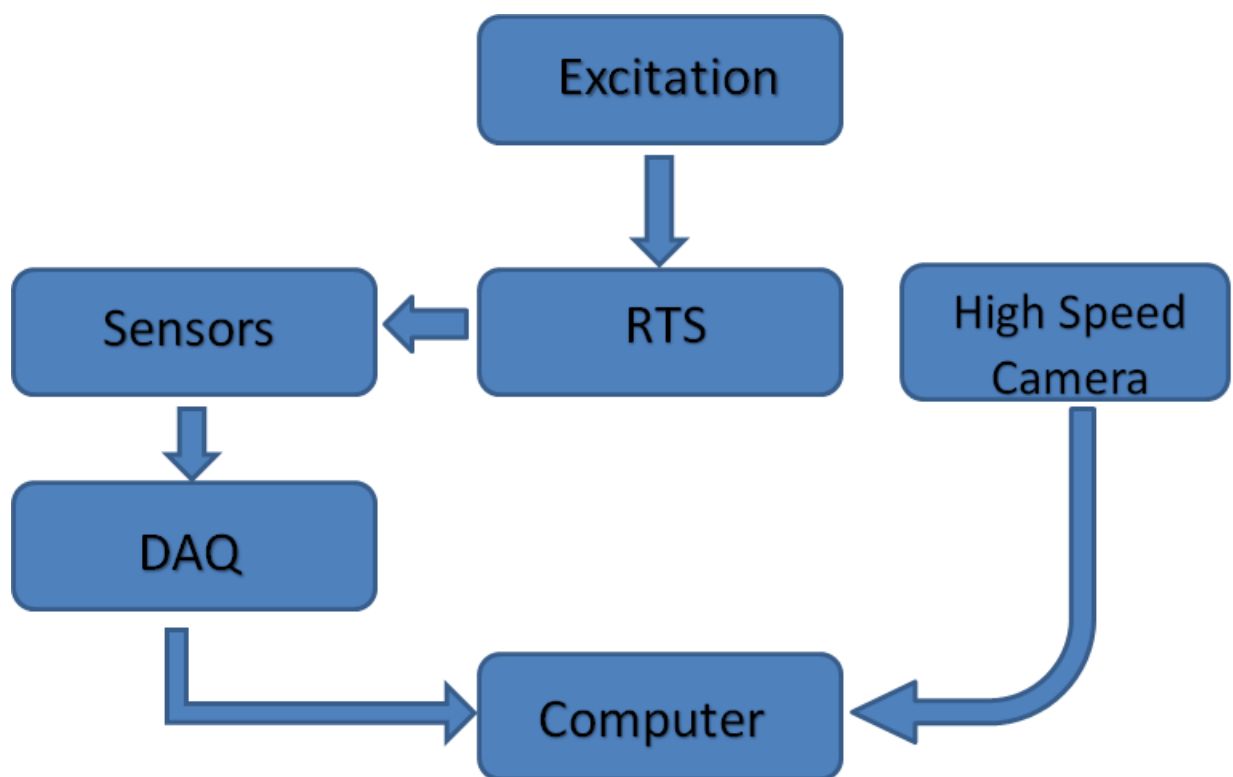


Figure 3.1: Schematic diagram of RTS experimental setup

Figure. 3.1 shows the schematic diagram of the Reciprocating test rig, which simulates the sloshing phenomenon under controlled excitation to measure dynamic force and dynamic acceleration on the tank wall and also dynamic pressure at the interface of fluid and tank walls. It also measures sloshing noise radiated from the tank. The system consists of four major subsystems which are servo motor with multi turn potentiometer, coupling disc which connects the motor shaft to the connecting rod and on which there is provision for variation of amplitude of excitation, base plate with bearings attached at bottom moving on guide

bars and rectangular tank with provision for sensor mounting

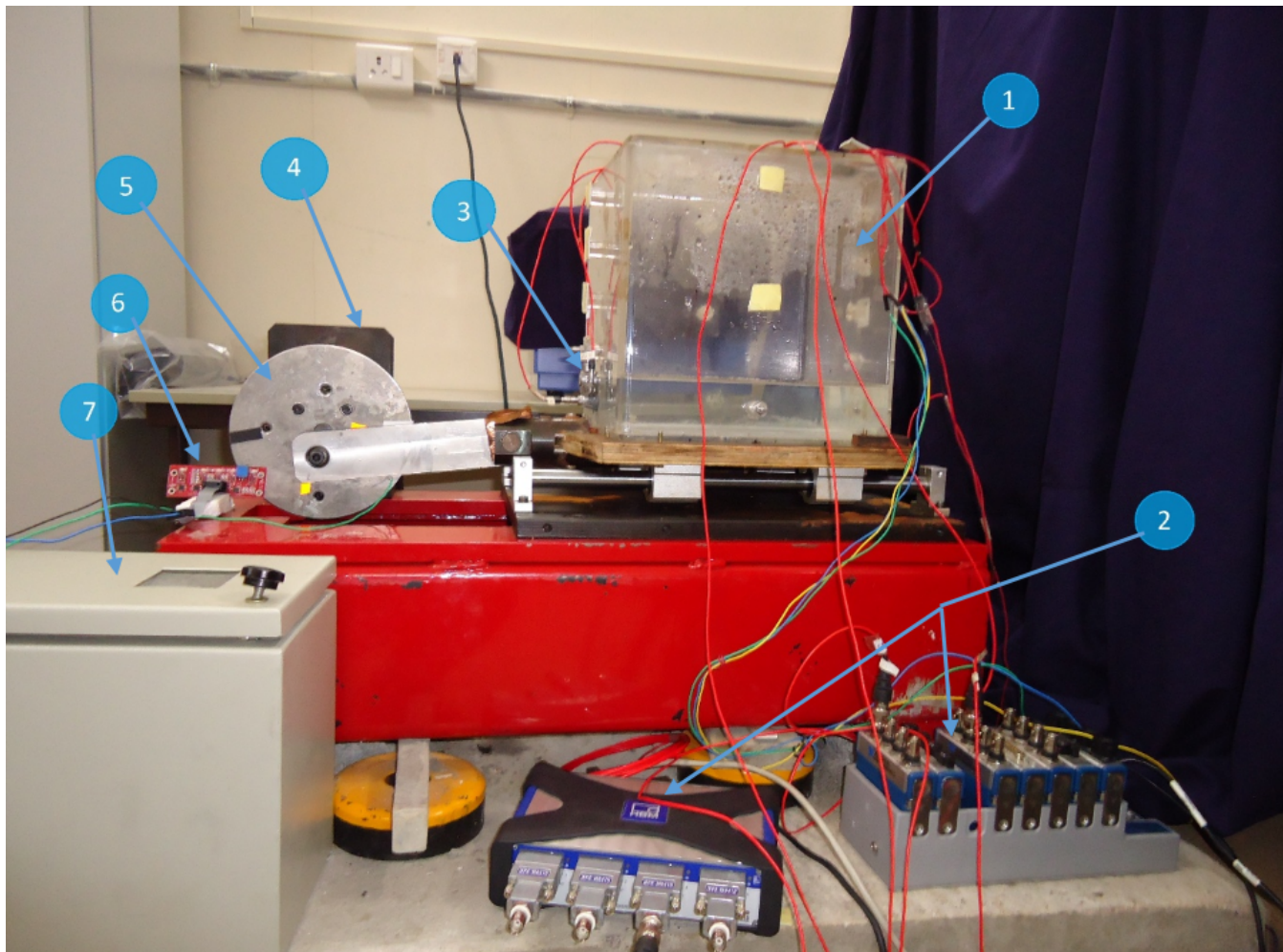


Figure 3.2: Reciprocating Test Rig (RTS) Experimental setup

3.1 Subsystem details

1. Rectangular tank with integration of sensors mounting

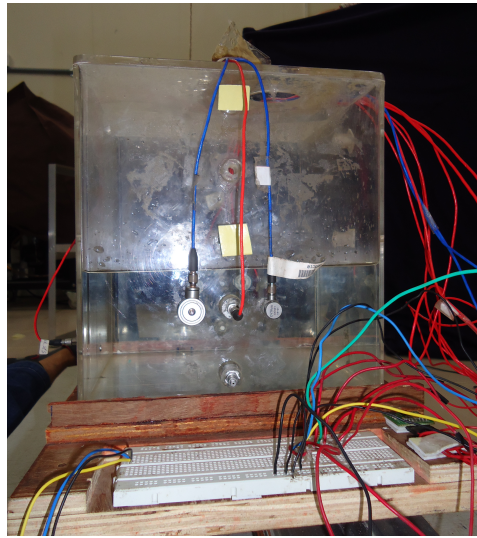


Figure 3.3: Acrylic tank with sensor mountings

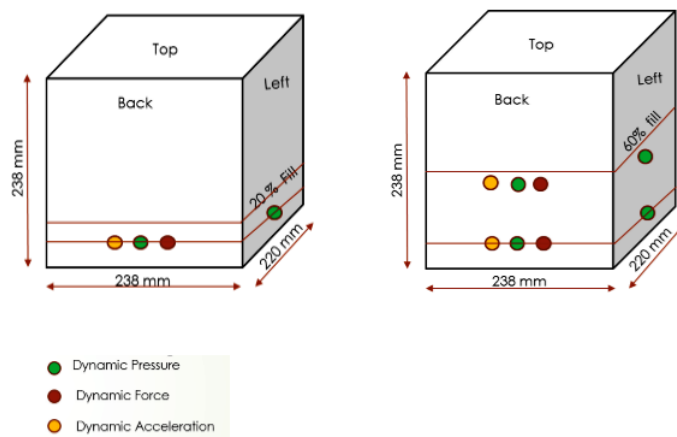


Figure 3.4: Schematic diagram of sensor mounting locations (a) 20 % fill (b) 60 % fill

Figure.3.3 shows, A transparent rectangular tank made of Acrylic was fabricated with a length of 238 mm, width of 220 mm and height of 238mm. The tank wall was 6 mm thick. This tank was placed over a wooden platform that was attached to quieter wheels in order to reduce background noise. The platform was maintained at a horizontal position with respect to the ground with the help of a spirit level. A three axis linear inertia acceleration sensor (3g-ADXL335) and a line triggering sensor were mounted on this platform. The inertia sensor is used to monitor vehicle acceleration and deceleration. Depending on the experimental

condition, the sensors can be mounted at 10 %, 30 %, 50 % and 70 % of tank height. Figure.3.4 shows, sensor mounting location for 20 % fill and 60 % fill level of tank height. Most of the dynamic action is observed mostly in front and back wall of tank, so dynamic force and dynamic acceleration sensors are mounted on those walls. As fluid comes directly in contact with dynamic pressure sensor, so to capture dynamic events at the wall and fluid interface, dynamic pressure sensors are mounted on front, back and top wall of the tank. Sloshing is surface wave phenomenon, to capture this, sensor location is fixed at 10 % below fill level. For example, suppose fill level is 60 % then the sensor height should be chosen as 50 % of tank height , sensors are also kept at constant 10 % height to see behaviour change at different fluid layers. At each sensor height position, dynamic pressure is mounted at centre and dynamic force and dynamic acceleration sensors are mounted besides to the dynamic pressure sensor.

2. Sensors integration with Data Acquisition

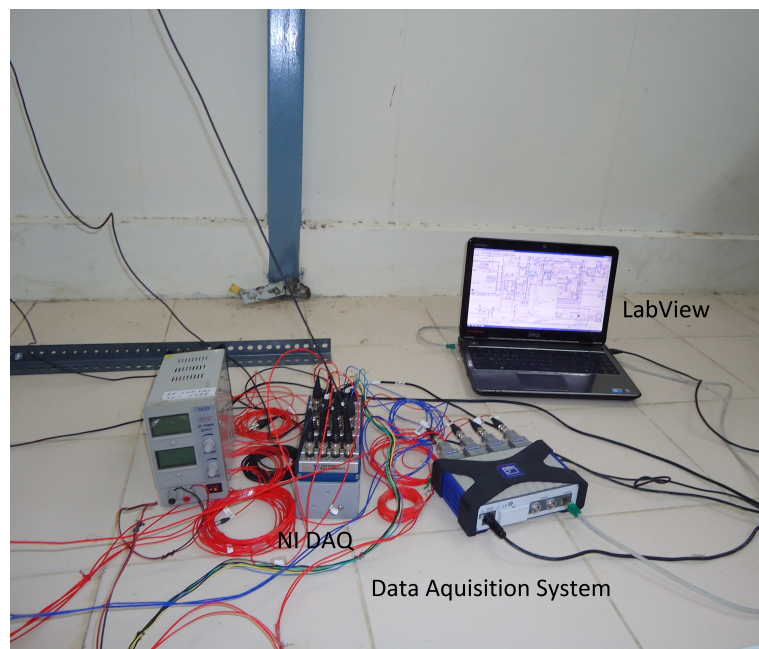


Figure 3.5: Data acquisition setup

- NI cDAQ-9178 data acquisition system

Figure. 3.6 shows schematic diagram of DAQ is being used as interface between sensors and LabView software.

Data from all sensors were acquired using a NI cDAQ-9178 data acquisition system which was triggered by the line sensor, which is in turn was activated by the color change on the coupling disc.

A customized Labview program was used to acquire the data from all the sensors.

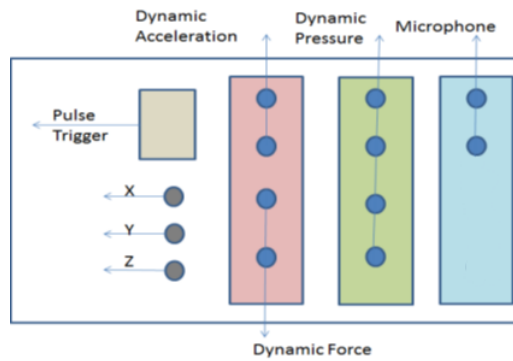


Figure 3.6: Schematic diagram of Data Acquisition system

Code extended to all the sensors and a way to synchronize the data from these sensors is been established.

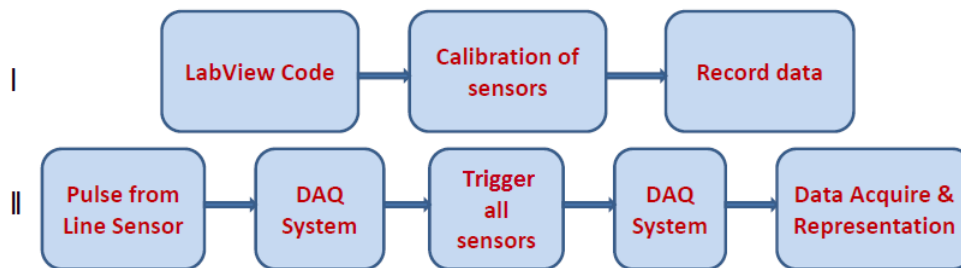


Figure 3.7: Schematic diagram of data acquisition process

- Dynamic force sensors : Figure. 3.8 (a) shows, dynamic force sensor. Dytran 1053V3 and Dytran 1051V4 models used to measure dynamic force on the wall of the tank. Sensitivity of the sensor used was 11.24 mV/N



Figure 3.8: Sensors used for data acquisition (a) Dynamic force (b) Dynamic acceleration (c) Microphones (d) High speed camera

- Dynamic acceleration sensors Figure 3.8 (b) shows the dynamic acceleration sensor. Dytran 3055B1 with sensitivity 10 mV/g. is used to measure the dynamic acceleration on wall.

- Microphones Figure 3.8 (c) shows the microphone used for experiment. BSWA MPA416 with sensitivity 60 mv/Pa, is used to record the radiated sound pressure level. two microphones are kept in front and top direction.

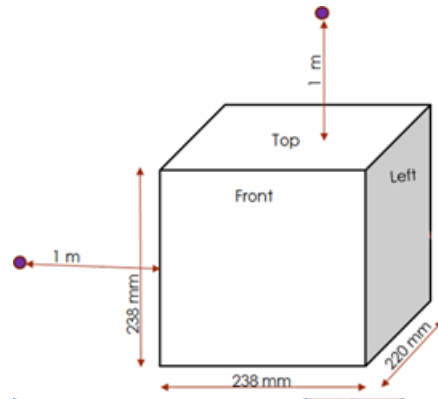


Figure 3.9: Schematic diagram of microphone position

To measure sound pressure level accurately, microphone should be kept in far field. The distance of far field is selected as per the discussion in section 2.4. By considering interested maximum frequency as 500 Hz, microphone is located at a distance of 1 m from the tank wall as shown in Figure 3.9.

- High speed camera

Figure. 3.8 (d) shows high speed camera- Phantom V12.1, used to capture the sloshing events inside the tank. 1000 fps frame rate was used to capture small sloshing moments. Camera is also triggered with rest of the sensors to make it possible to compare all the data with respect to the same time frame.

Depending on the experimental condition, the sensors can be mounted at 10 %, 30 %, 50 % and 70 % of tank height as shown in Figure. 3.4. An extensive study was conducted to determine repeatability of the test data. Parametric studies were conducted with varying fill levels and sensor locations.

Chapter 4

Numerical Analysis

4.1 Fluid Structure Interaction (FSI) coupling

In FSI simulation, usually structure deforms due to forces caused by fluid flow. The deformation must be transferred to CFD code which corresponds to quantity nodal position while the pressure and forces are sent from CFD to structural code. MpCCI is a tool to perform multiphysics computations by coupling independent simulation codes. MpCCI (Multi-Physics Code Coupling Interface) is used as coupling tool between CFD solver (STAR-CCM+) and Structural solver (Ansys). MpCCI is a software environment which enables the exchange of data between the meshes of two simulation codes in a multiphysics simulation. MpCCI enables a direct communication between the coupled codes by providing adapters for each code.

4.2 Co-Simulation Methodology

FSI co-simulation follows the following steps [?] :

1. Preparation of Model files:

Before starting the simulation, model file created in each code i.e. here STAR CCM+ and ANSYS. Model contains definition, coupling region and other analysis information.

2. Defining of coupling process:

After importing the two models in MpCCI environment then the coupling region i.e. specific region which are taking part in actual data transfer in MpCCI are defined. Also the quantities to be transferred are set. For this simulation overpressure data is exchanged from STAR CCM+ to ANSYS and the nodal position data is exchanged from ANSYS to STAR CCM+. Overpressure is the gauge pressure or the absolute pressure minus the atmospheric pressure. Number of time steps, iteration etc. information is defined in coupling process.

3. Running Co-simulation:

After starting the MpCCI server both coupled codes are started. Each code computes its part of the problem while the MpCCI controls the quantity exchange i.e. overpressure and node position.

4. Post processing:

After the co-simulation, the results are analyzed with the post-processing tools of each simulation code i.e. STAR CCM+ and ANSYS for this case.

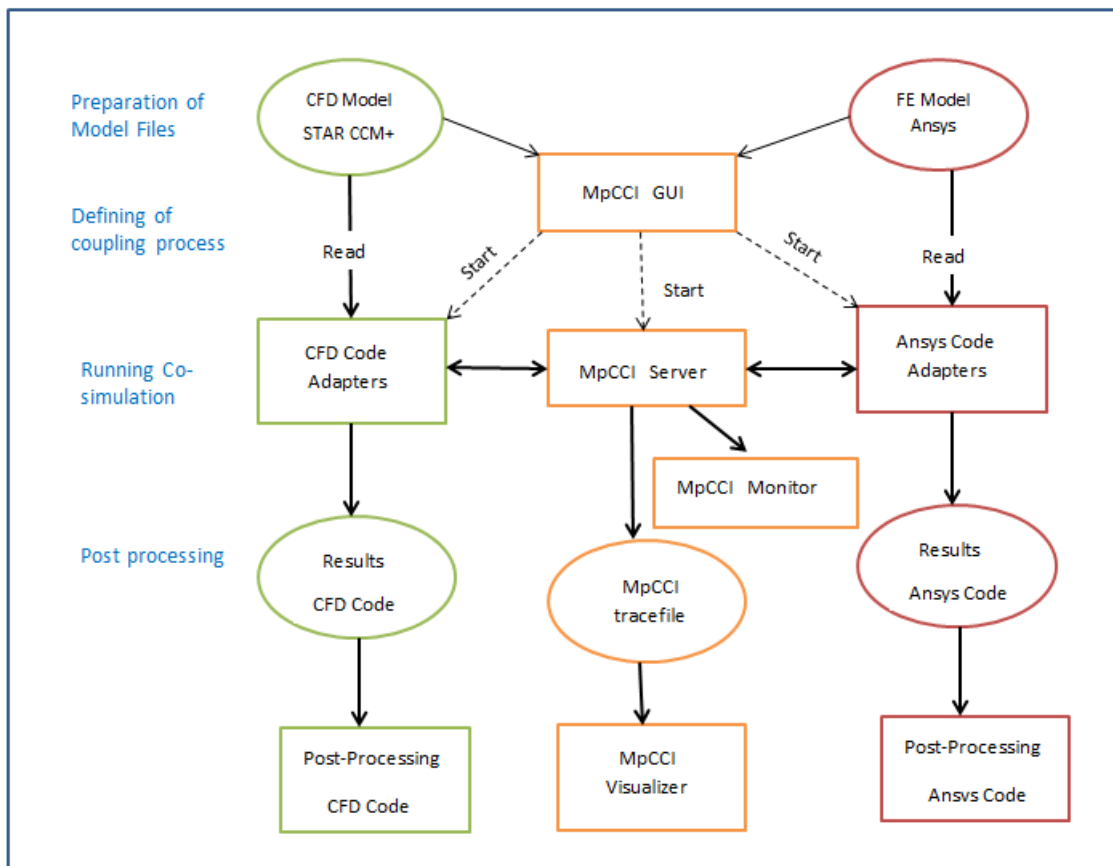


Figure 4.1: Flowchart of co-simulation methodology in MpCCI

4.3 Sloshing Noise Prediction Methodology

Figure.4.2 shows Sloshing Noise generation mechanism. Based on the structural flexibility of the wall, the problem can be solved either as one-way coupled or two-way coupled FSI problem. This can be used to determine the dynamic pressure and corresponding wall displacement. This vibration displacement acts as a boundary condition in the acoustic

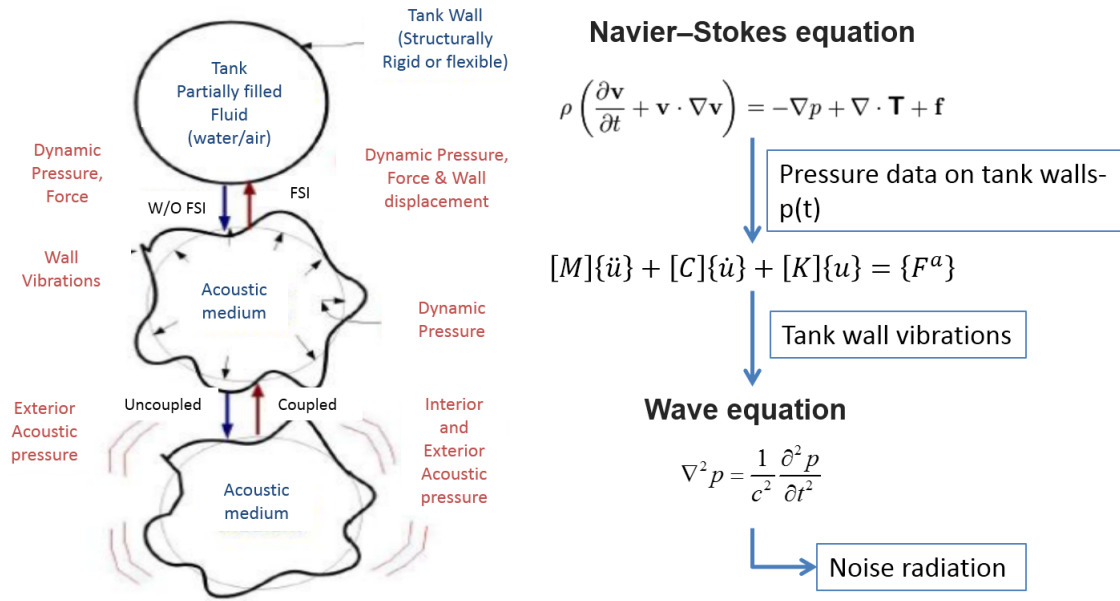


Figure 4.2: Sloshing Noise generation mechanism

analysis. Similarly, in acoustic analysis the tank can be modelled as acoustically rigid or flexible. If the tank is acoustically flexible, then it can be modelled as acoustic-structural coupled problem.

Figure. 4.3 shows the one-way coupled approach for noise generation in time and frequency domain.

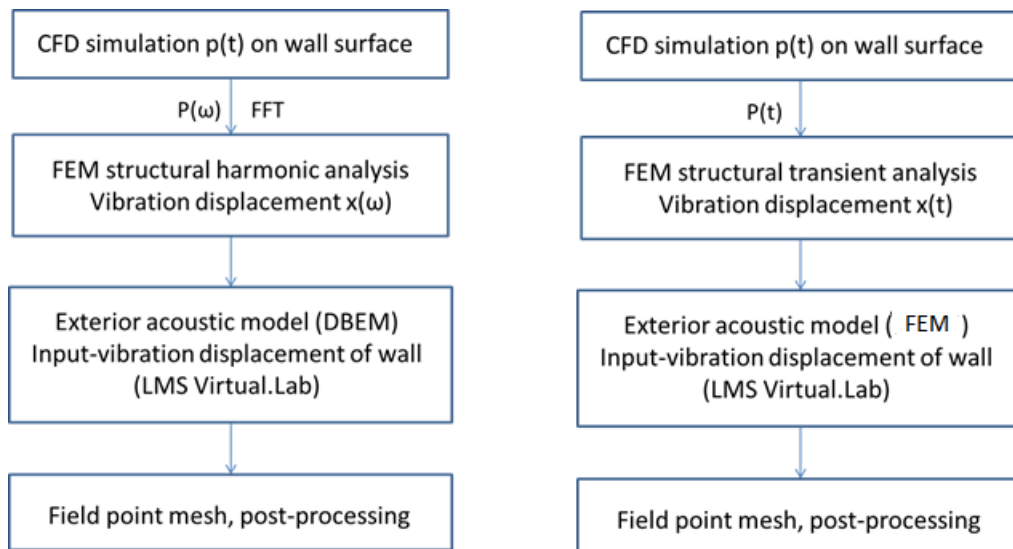


Figure 4.3: Tank sloshing simulation methodology

Displacement in time domain is determined by applying a transient pressure on structural wall. Similarly, using Fast Fourier Transform (FFT) on transient pressure data from

CFD, pressure in frequency domain is determined. It is applied as excitation to the structural wall and corresponding harmonic displacement is calculated by doing harmonic FEM analysis. These displacements are used as acoustic boundary conditions in corresponding acoustic transient FEM and acoustic harmonic BEM analysis. Propagating sound pressure level is determined at defined field point locations.

As mentioned before, noise generated due to liquid sloshing is categorized into three types of noise sources, which are Clonk, Hit and Splash Noise. Clonk and Hit noise dominates the frequency range of 50 Hz to 2000 Hz and Splash noise is dominant in the higher frequency range of 500 Hz to 10 kHz range. The splash noise is due to the liquid-liquid interaction. The current proposed Vibro-acoustic model will not compute splash noise.

The frequency domain approach can be performed by taking pressure loading on tank walls from computational fluid dynamics (CFD) study. This approach is valid for linear sloshing regime where it is assumed that the change in the liquid center of gravity is negligible. However, it may not be true for higher deceleration loading. Hence, it is required to consider a time domain approach for nonlinear sloshing. Nonlinear sloshing predominates for higher deceleration loading or higher fill levels. The current analysis assumes that the tank walls are acoustically rigid and therefore one-way coupling was considered.

4.4 Structural Simulation

Modal analysis is performed in order to demonstrate the contribution of the structural properties of the tank in the slosh noise prediction. In this part of the present investigation the linear isotropic material (Acrylic) is used. Shell 63 element used to mesh the wall surface area and there are 29,000 shell elements as shown in Figure. 4.4 for the fuel tank. Following material properties is used for structural analysis, modulus of elasticity $2.1 \times 10^9 \text{ N/m}^2$, Poisson's ratio is 0.4 and density 1100 kg/m^3 . To take care of the effect of fluid on structural dynamics, fluid 80 elements are used to model the fluid in the tank. The structural shell element has a four-node element with six degrees of freedom for each node. Fluid element has eight nodes having three translation degrees of freedom for each node. The displacement of shell and fluid elements of the tank wall is coupled in the normal direction. During sloshing the fluid inside the tank is divided into two parts i.e. sloshing mass which causes most of the dynamic activities and rigid mass which gives mass loading effect. During sloshing, the percentage of sloshing mass is less compared to rigid mass specially at higher fill levels. Thus an assumption is made that the dynamic mass is very less compared to rigid mass and the whole fluid mass is modelled as rigid mass in the FEA modelling.

Acoustic boundary element model of tank volume has to be created. The acoustic boundary element size is determined by the wavelength of the highest frequency of interest. At least six elements per wave length are required for the simulation [?]. Assuming that

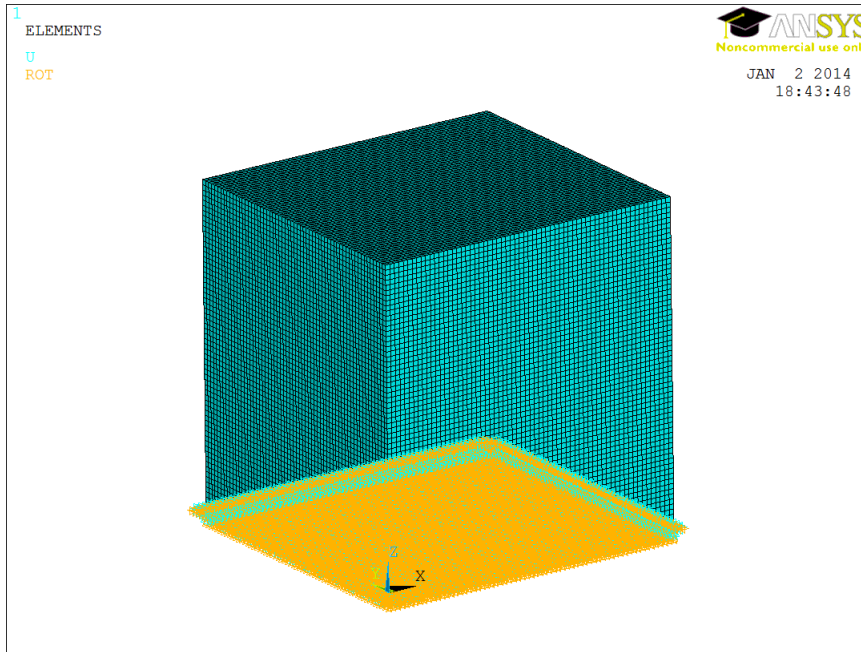


Figure 4.4: Structural analysis model

the sound is traveling through air at standard temperature and density, Table 4.1 shows the highest frequency and the recommended element size for the simulation.

Table 4.1: Maximum frequency and recommended element size

Maximum Frequency(Hz)	Recommended element size(mm)
500	113
1000	57
1500	38
2000	28
2500	23

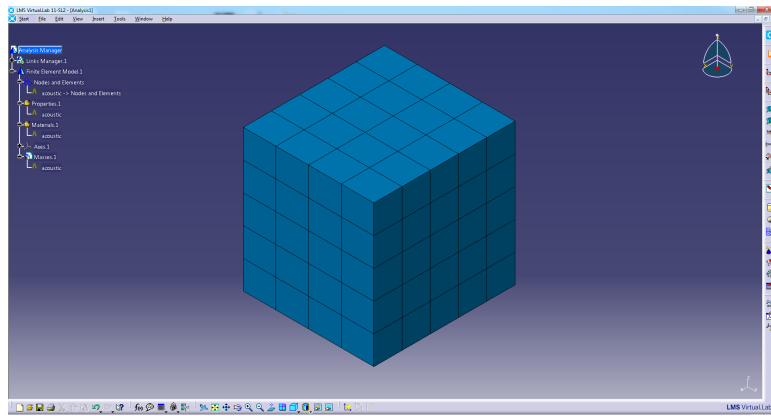


Figure 4.5: Acoustic analysis model

Chapter 5

Results and discussion

5.1 Experimental Analysis

Following conditions and assumptions are considered through out the experiment.

1. Excitation is sinusoidal i.e. periodic in nature
2. All sensors are triggered from the same crank angle of rotation i.e. 135° from IDC.
3. Microphone locations are fixed at 1m distance from each of the side wall and top wall of tank.

5.1.1 Parametric Study

During initial experimental trials, it was observed that the fluid sloshes violently and maximum dynamic activities are observed on the tank walls when the external excitation force is equal to the sloshing natural frequency of the fluid. This is the nonlinear sloshing behaviour and only hitting phenomenon is observed. As the external excitation frequency is reduced we observe weakly non linear sloshing at $0.75*f_s$ and linear sloshing at $0.5*f_s$ (f_s is sloshing natural frequency). Also it was observed that when the external excitation frequency was two times the sloshing natural frequency i.e. $2*f_s$ only splashing phenomenon was observed. Thus, based on the above observations following parametric studies have been conducted to understand the sloshing behavior at different fill level and excitations.

Table 5.1: Parametric Study

Parameters	Range
Fill Level (%)	10,20,30,40,50,60,70,80
Excitation Frequency (Hz)	$0.5*f_s$, $0.75*f_s$, $1*f_s$, $1.25*f_s$, $1.5*f_s$, $2*f_s$
Sensor Location	10% below fill level (Fixed)
Amplitude of excitation	20 mm (Fixed)

5.1.2 Sloshing Natural Frequency Estimation - Analytical, Experimental and Numerical

1. Analytical Method

Sloshing natural frequency depends on the geometry of the tank and fill level. Sloshing natural frequency for rectangular tank is given by,

$$\omega_n^2 = (2n + 1)\pi(g/L) \tanh((2n + 1)\pi h/L) \quad (5.1)$$

Where,

L - dimension of the base of the tank along sloshing direction

h - height of the fluid filled in the tank

g - acceleration due to gravity

n - mode number n=1,2,3,..

2. Experimental Method

When a partially filled tank is excited the fluid starts to oscillate. The oscillations may be nonlinear, weakly nonlinear or linear depending on the excitation which are defined as:

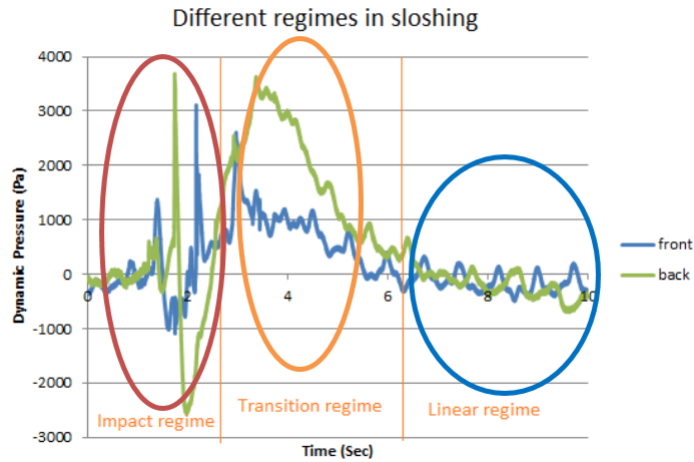


Figure 5.1: Sloshing Regimes

Nonlinear sloshing: Strongly nonlinear motion where the nonlinearity is mainly due to rapid velocity changes associated with hydrodynamic pressure impacts of the liquid motion close to the free surface.

Weakly nonlinear sloshing: Relatively-large-amplitude oscillations in which the free liquid surface experiences nonplanar motion.

Linear sloshing: Small oscillations in which the fluid free surface remains planar.[?]

Sloshing time period is calculated in the linear sloshing zone from pressure sensor readings. Experimental sloshing time period is the time between two peaks in the pressure sensor measurements.

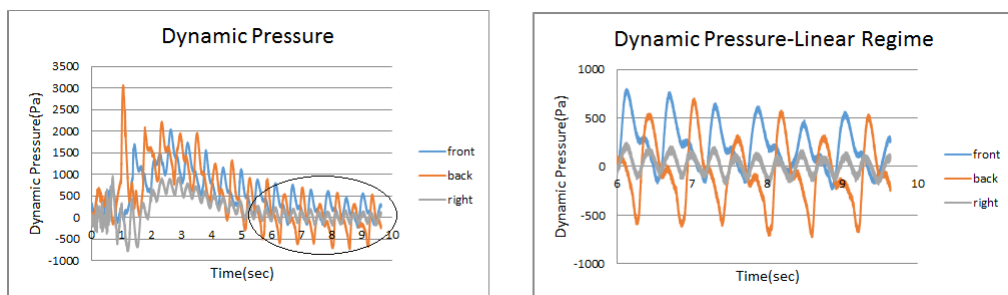


Figure 5.2: Experimental Sloshing Frequency calculation from dynamic pressure data

3. Numerical Method

The volume of fluid is modelled using Fluid80 elements. Displacements of fluid elements near tank walls are constrained in normal direction to simulate rigid tank walls. Acceleration due to gravity is included. Mode extraction method used for modal analysis is Reduced method.

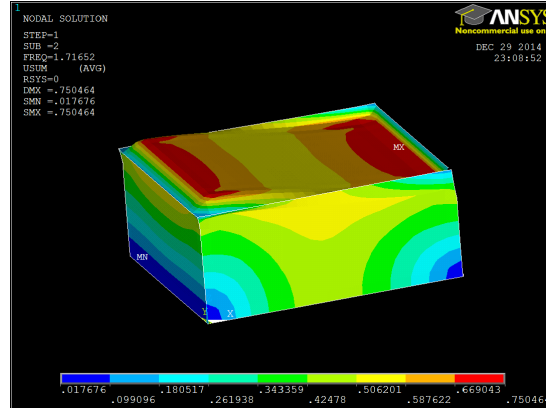


Figure 5.3: Sloshing mode calculated based on Numerical analysis

The figure shows first mode for 40 % fill level of water.

4. Comparison of sloshing natural frequency using different methods:

Table 5.2: Sloshing Natural Frequency Comparison

Fill Level	Sloshing natural frequency (Hz)		
	Theoretical	Experimental	Numerical
20 %	1.35	1.32	1.39
40 %	1.67	1.61	1.71
60 %	1.77	1.75	1.78
80 %	1.80	1.82	1.84

Table5.2 shows sloshing natural frequency calculated using different methods.

Table5.2 shows that the sloshing natural frequency in the linear zone is well comparable using theoretical, experimental and numerical methods. This values of sloshing natural frequency is used to calculate the external excitations for the parametric studies. Thus, the analytical formulae available for sloshing natural frequency, wave height, dynamic pressure and dynamic force are valid only in linear zone. But for nonlinear zone dynamic pressure and dynamic force can be experimentally measured.

5.1.3 Modal Analysis

Modal analysis of tank was done with varying fill levels to check the effect of fill level on dynamic response of tank.

1. Experimental modal analysis

Natural frequency of the tank is estimated by measuring drive point FRF.

The tank is fixed at the bottom.

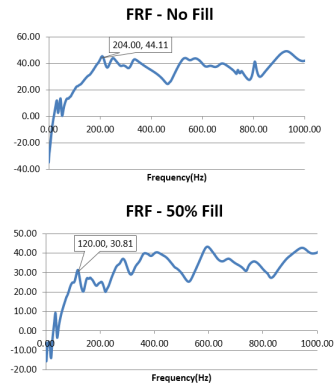


Figure 5.4: FRF for experimental modal analysis

The drive point frequency response function(FRF) graphs for empty and 50% filled tank is shown in figure 5.4 The FRF clearly shows that the natural frequency of tank reduces as fill level increases.

2. Numerical modal analysis.

Elements used for modelling the tank walls is SHELL 181 and water is modelled using FLUID 80. At fluid structure interface, nodes are coupled in normal direction to simulate fluid structure interaction. Fixed boundary condition is used for the tank base. Mode extraction method used is Block Lanczos.

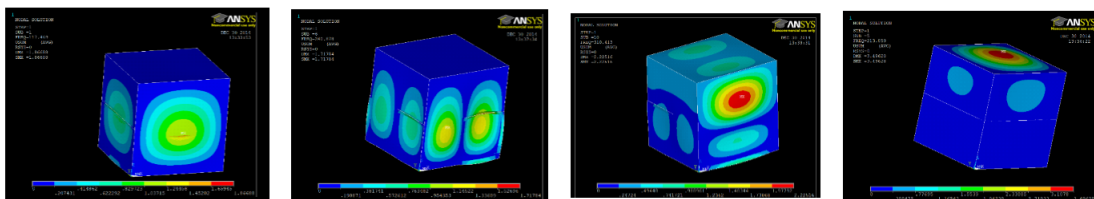


Figure 5.5: Numerical modal analysis

Figure 5.5 shows mode shape results for 50% fill level.

3. Comparison of experimental and numerical natural frequency.

Table 5.3: Effect of fill level on tank natural frequency

Fill Level(%)	Numerical(Hz)	Experimental(Hz)
0	197.19	207
10	195.3	210
20	193.8	200
30	183.13	174
40	142.49	140
50	114.41	116
60	106.19	100
70	82.112	84
80	74.2	82
90	68.15	78

Table 5.3 shows the natural frequency of the tank for various fill levels computed numerically and experimentally.

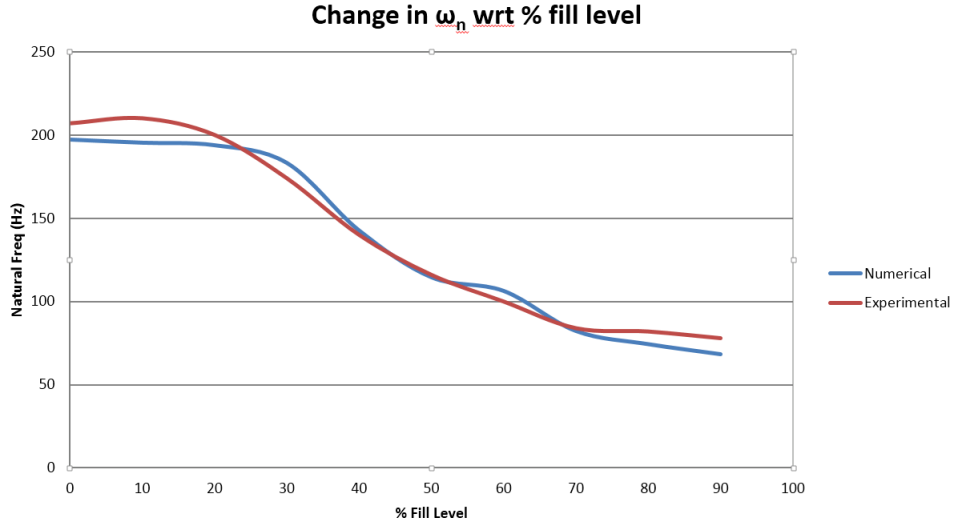


Figure 5.6: Effect of fill level on tank natural frequency

Figure 5.6 clearly shows that natural frequency of tank decreases with increasing fill level and experimental and numerical results are in good agreement.

The change in the natural frequency of the tank is investigated to check the effect of fluid mass as an influencing factor.

Natural frequency is given by:

$$f = \frac{1}{2\pi} \left(\sqrt{\frac{k}{m}} \right) \quad (5.2)$$

Where,

f=Natural frequency (Hz)

k=Stiffness (N/m)

m=Mass (kg)

Thus,

$$\left(\frac{f_2}{f_1}\right)^2 = \frac{m_1}{m_2} \quad (5.3)$$

If the above equation is satisfied then it can be concluded that the change in natural frequency is due to mass loading effect of the fluid.

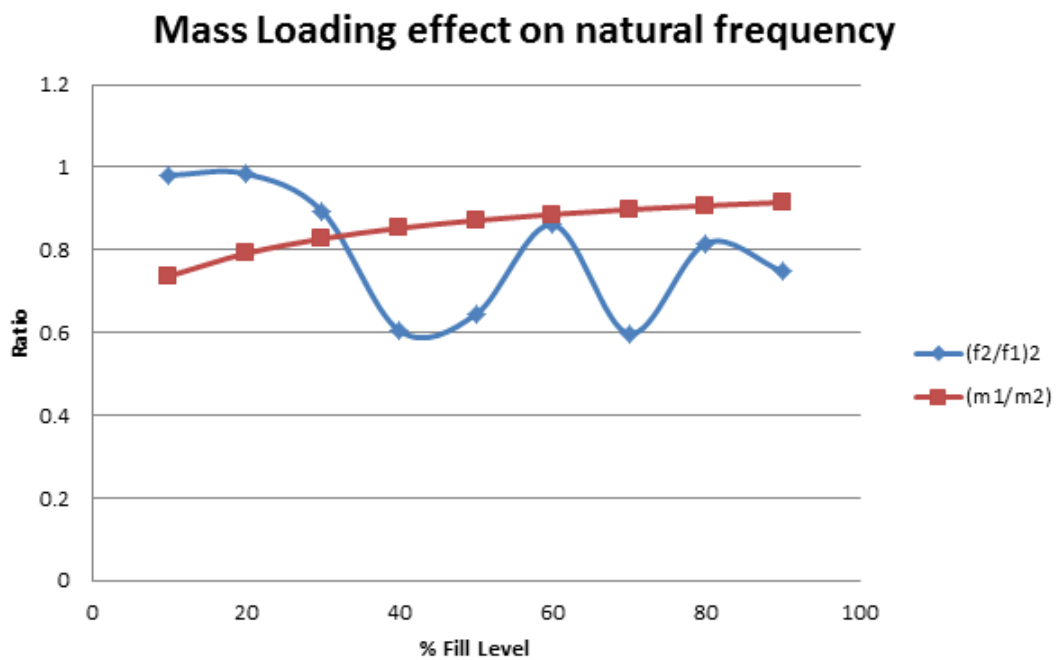


Figure 5.7: Mass Loading Effect on tank natural frequency

Figure 5.7 shows the plot of the ratio of frequency vs ratio of total mass for various fill level. It can be concluded that the ratio of frequencies is nearly equal to the ratio of masses and thus mass has more effect than stiffness on the change in natural frequency of tank with increase in fluid fill level in the tank.

5.1.4 Experimental Results

20% Fill

$0.5 f_s$

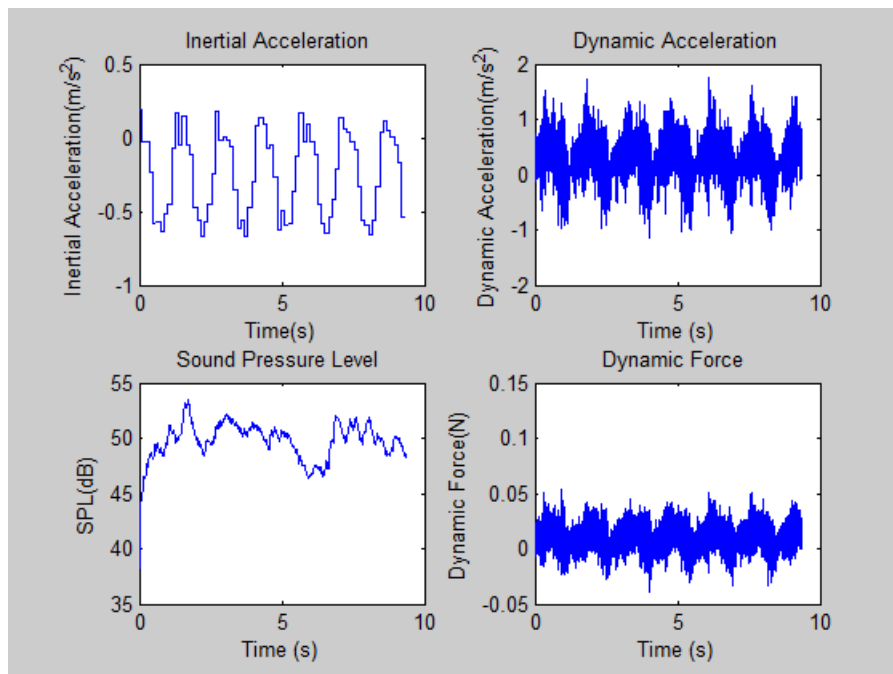


Figure 5.8: 20% Fill 0.5 fs

The figure 5.8 shows the inertial acceleration, dynamic acceleration, dynamic force and noise experimental measurements. The results show that the measurands are repeatable for each cycle. Also it is seen that noise generation is synchronous with dynamic acceleration and dynamic force peaks. Thus it can be seen that the dynamic activities happen at the same time.

$0.75 f_s$

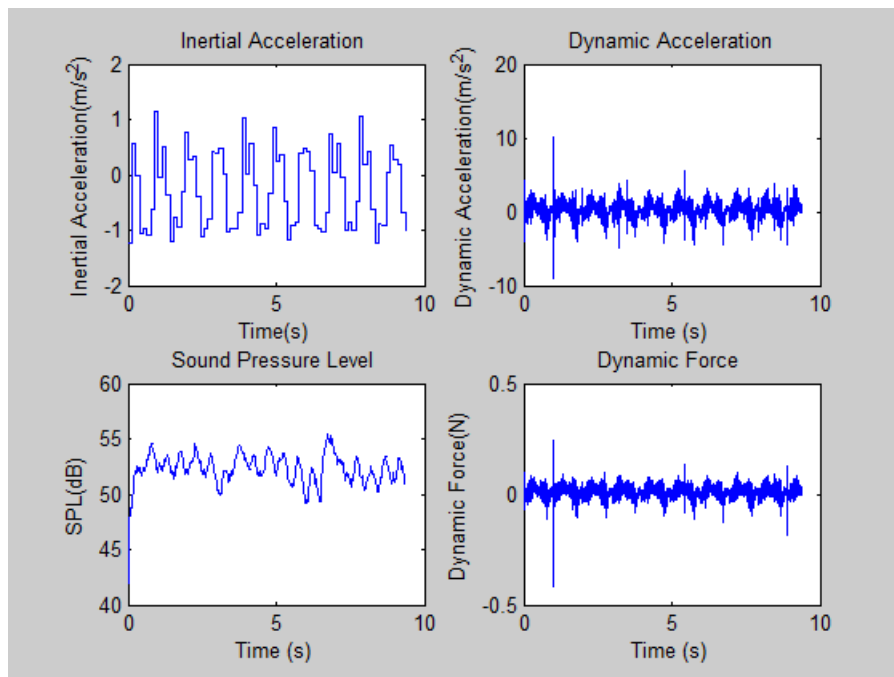


Figure 5.9: 20% Fill 0.75 fs

$1 f_s$

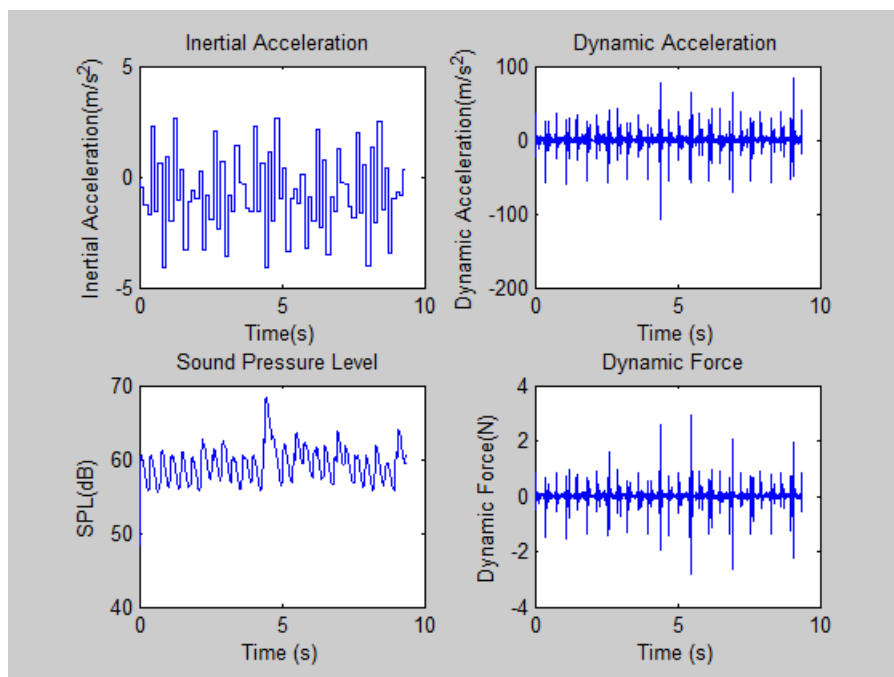


Figure 5.10: 20% Fill 1 fs

1.25 f_s

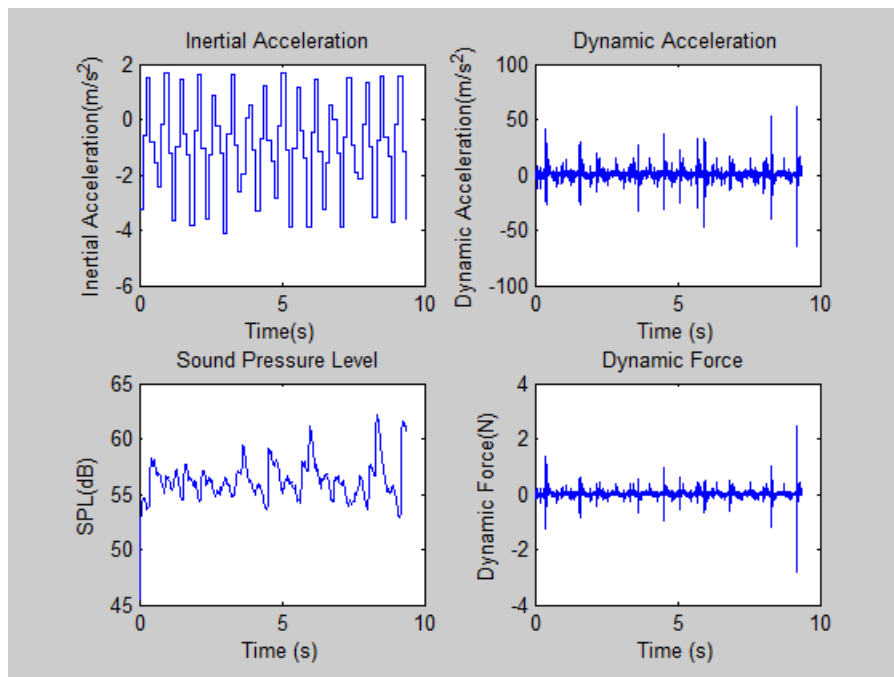


Figure 5.11: 20% Fill 1.25 fs

1.5 f_s

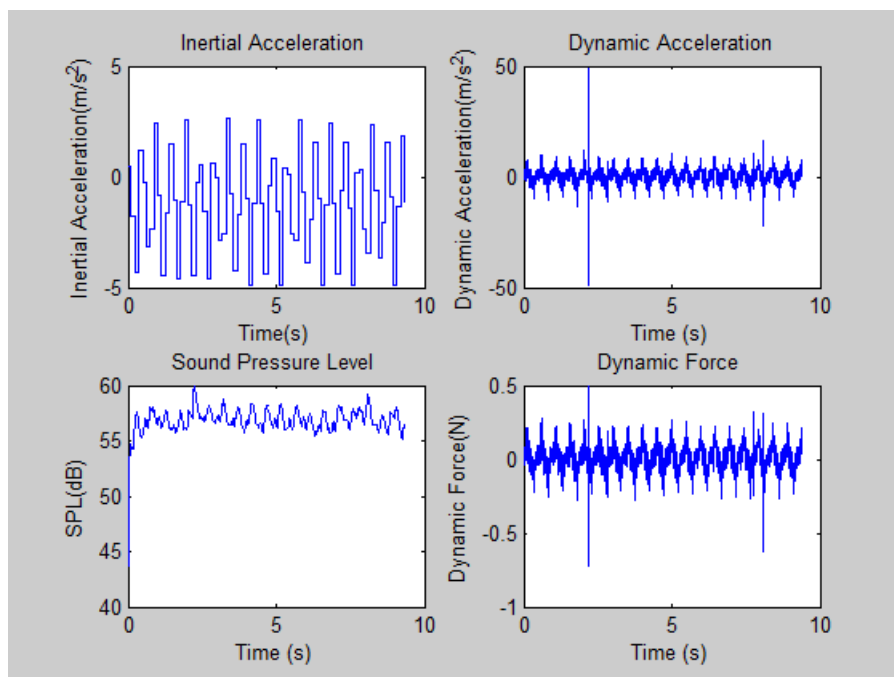


Figure 5.12: 20% Fill 1.5 fs

$2 f_s$

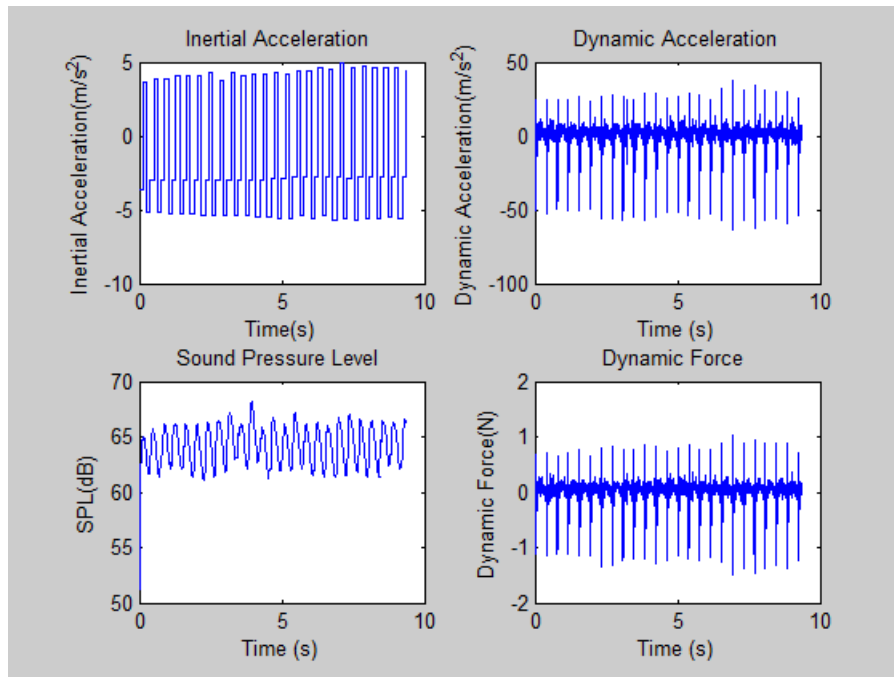


Figure 5.13: 20% Fill 2 fs

The above results show that inertial acceleration, dynamic acceleration, dynamic force and noise experimental measurements. The results show that the measurands are repeatable for each cycle. Also it is seen that noise generation is synchronous with dynamic acceleration and dynamic force peaks. Thus it can be seen that the dynamic activities happen at the same time. Also, the dynamic activities increase as the excitation frequency nears the sloshing natural frequency i.e. 1 fs. At this excitation hitting noise is observed. When the excitation frequency is 2 fs dynamic activities at tank walls are less, but noise is still generated suggesting that it is splashing noise.

40% Fill

$0.5 f_s$

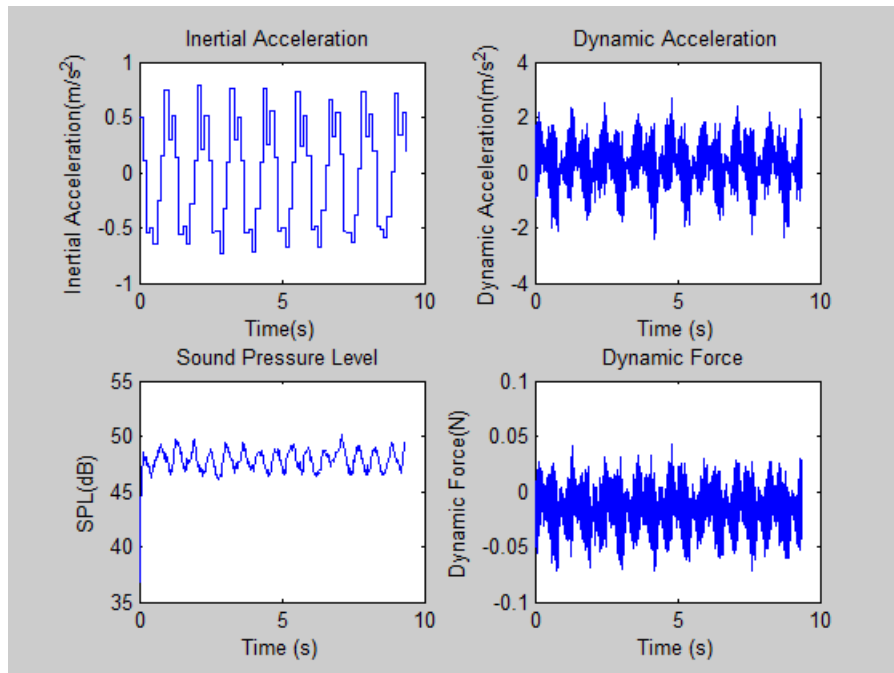


Figure 5.14: 40% Fill 0.5 fs

$0.75 f_s$

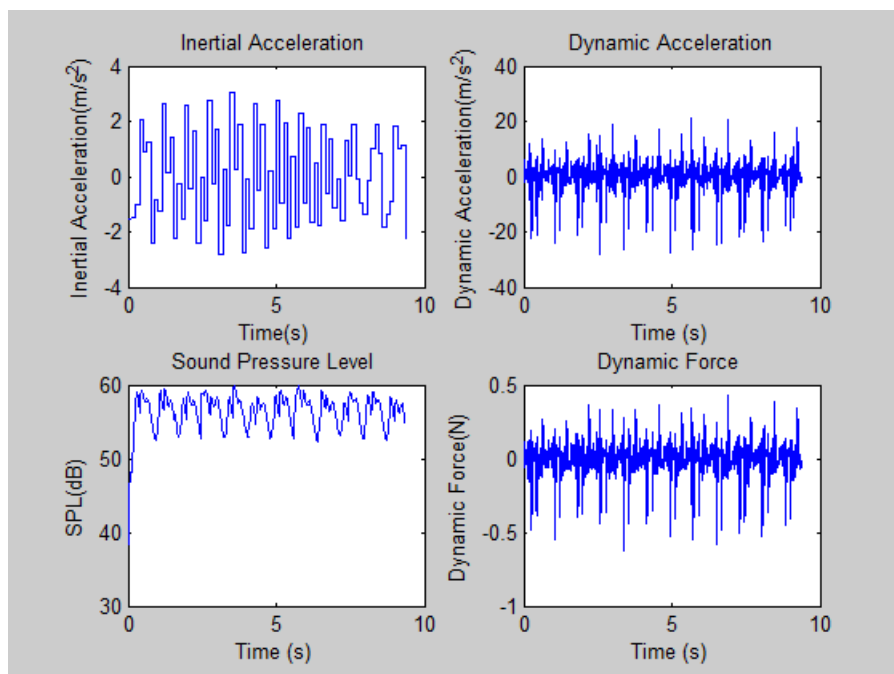


Figure 5.15: 40% Fill 0.75 fs

1 f_s

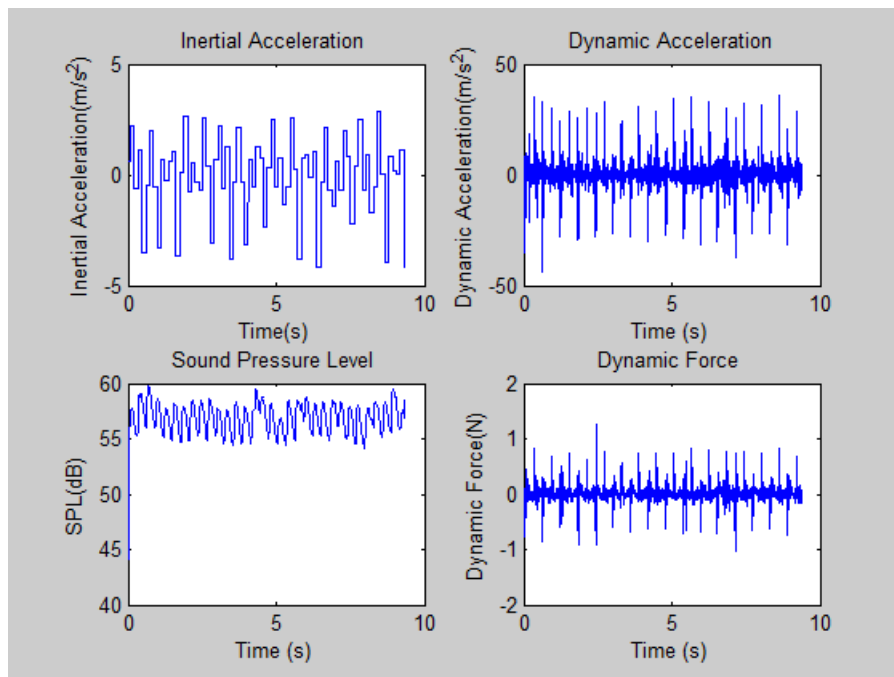


Figure 5.16: 40% Fill 1 fs

1.25 f_s

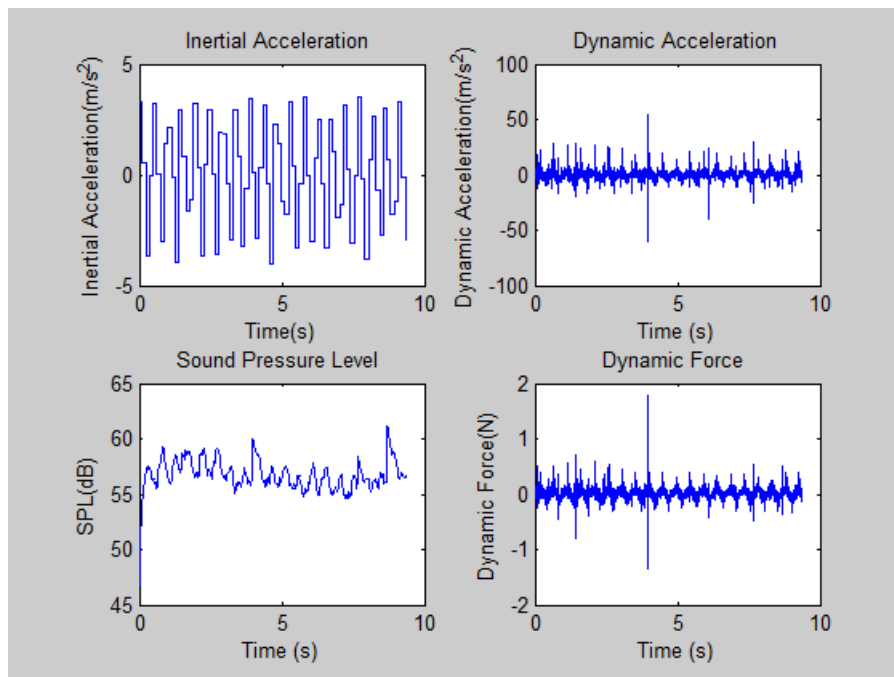


Figure 5.17: 40% Fill 1.25 fs

1.5 f_s

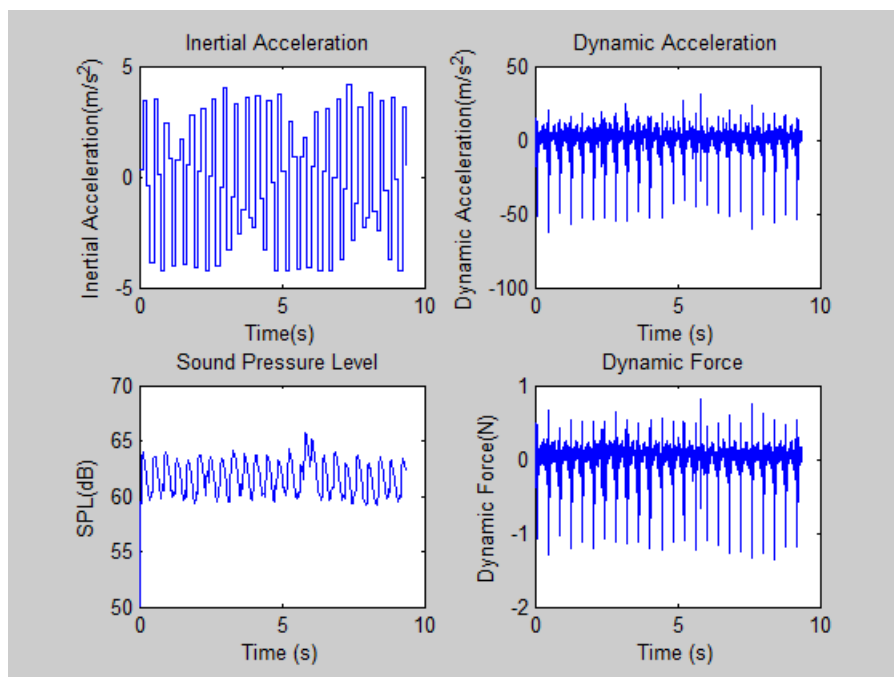


Figure 5.18: 40% Fill 1.5 fs

$2 f_s$

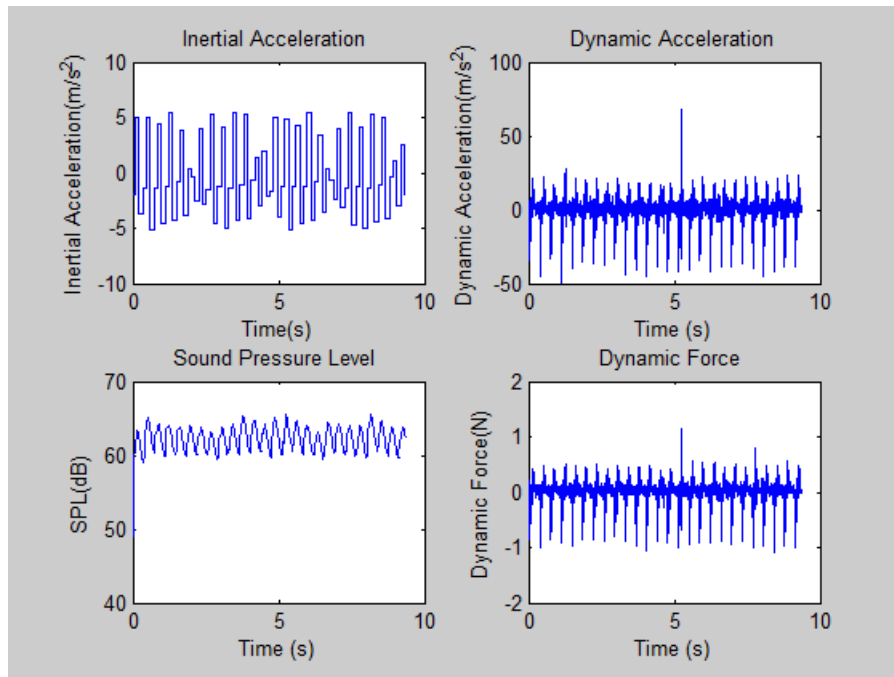


Figure 5.19: 40% Fill 2 fs

The above results show that inertial acceleration, dynamic acceleration, dynamic force and noise experimental measurements. The results show that the measurands are repeatable for each cycle. Also it is seen that noise generation is synchronous with dynamic acceleration and dynamic force peaks. Thus it can be seen that the dynamic activities happen at the same time. As the excitation frequency nears the sloshing natural frequency, hitting is observed at front, back and top walls.

60% Fill

$0.5 f_s$

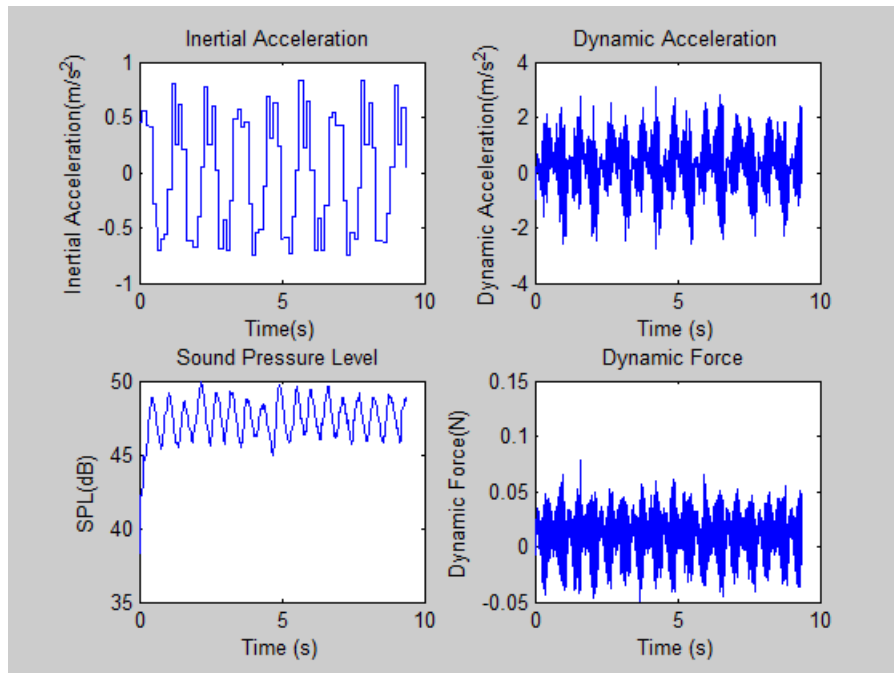


Figure 5.20: 60% Fill 0.5 fs

$0.75 f_s$

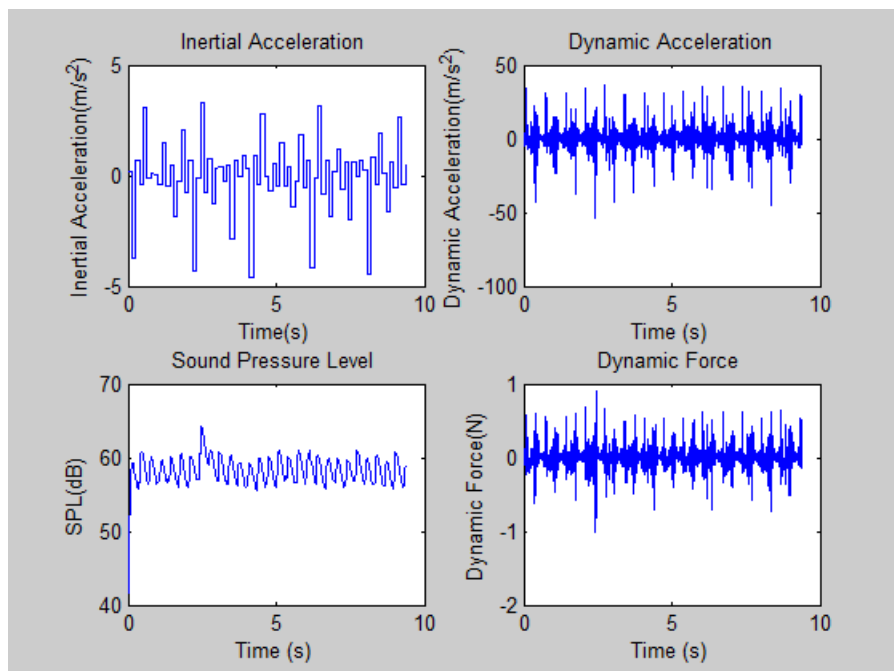


Figure 5.21: 60% Fill 0.75 fs

1 f_s

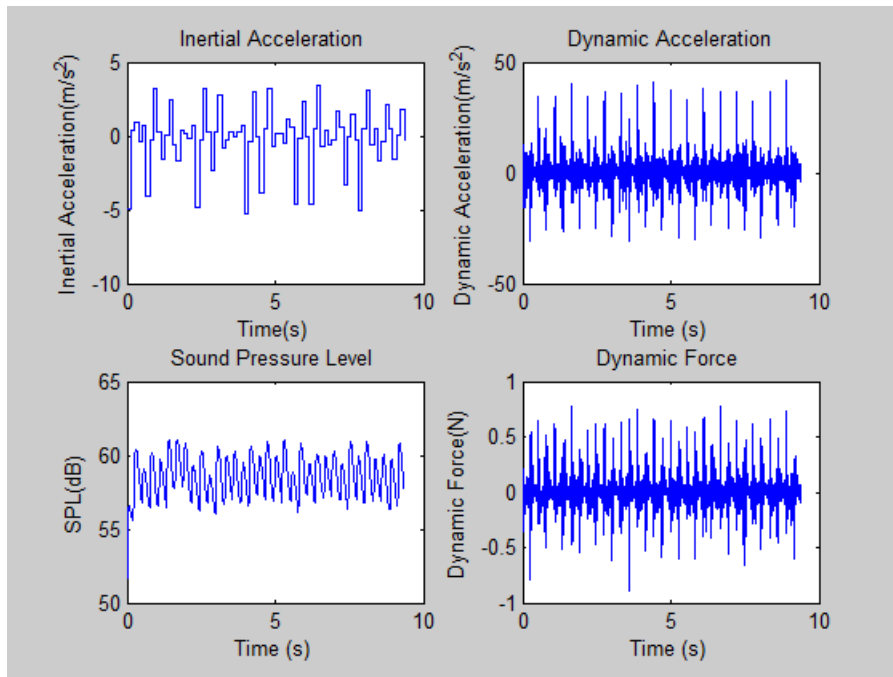


Figure 5.22: 60% Fill 1 fs

1.25 f_s

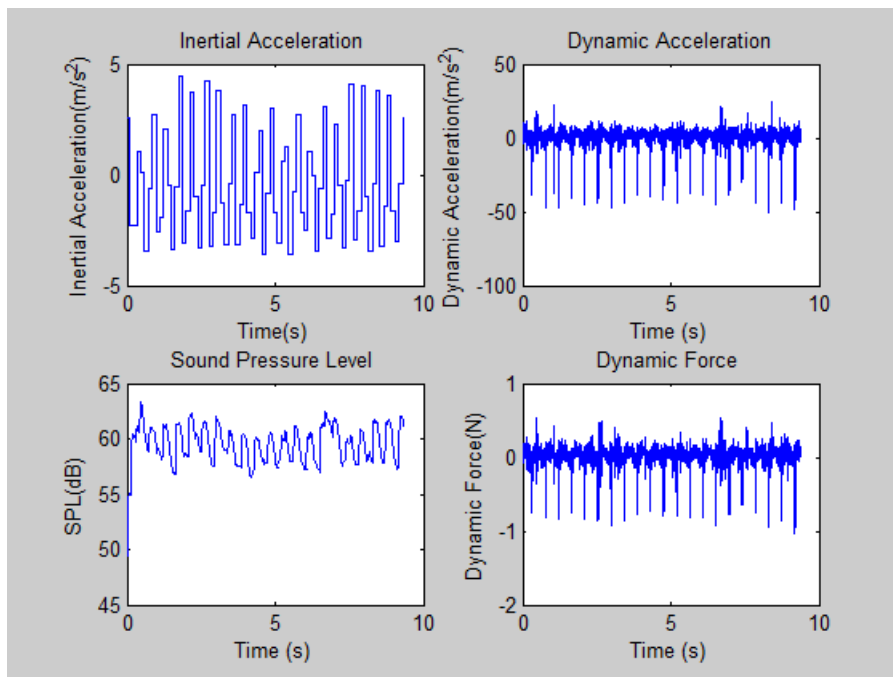


Figure 5.23: 60% Fill 1.25 fs

1.5 f_s

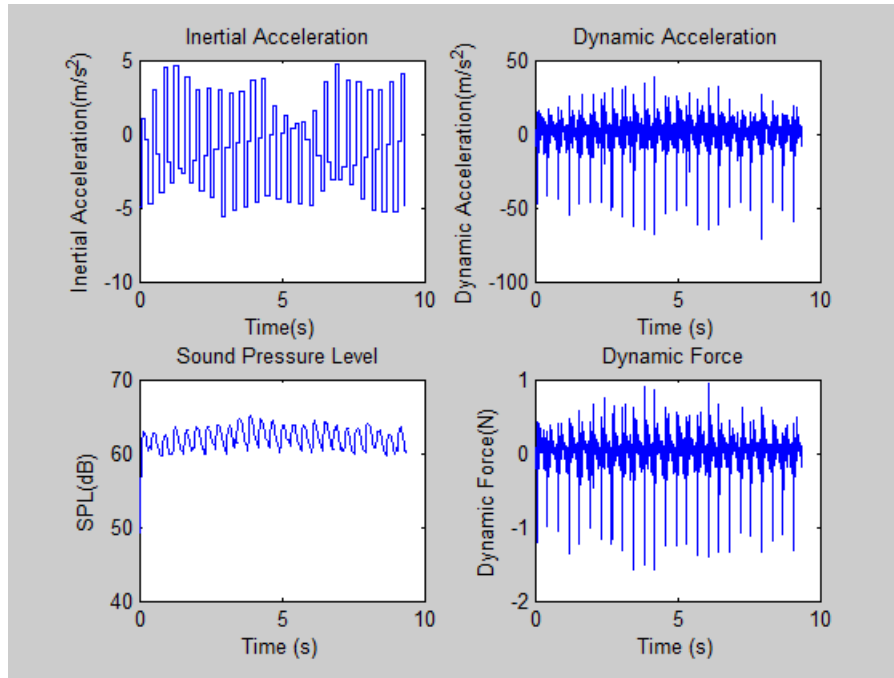


Figure 5.24: 60% Fill 1.5 fs

The above results show that inertial acceleration, dynamic acceleration, dynamic force and noise experimental measurements. The results show that the measurands are repeatable for each cycle. Also it is seen that noise generation is synchronous with dynamic acceleration and dynamic force peaks. Thus it can be seen that the dynamic activities happen at the same time. Here the dynamic activities happen more at the top wall compared to the front and back wall. At 1 fs, hitting is observed at the top wall. Also, splashing is observed. Thus, the noise is a combination of hitting and splashing.

Estimation of background noise

Before starting the experiment, it is important to estimate background noise. In first case, tank is filled with water and run on RTS setup, and corresponding sloshing noise, dynamic acceleration and dynamic force is recorded. While in second case water in tank is replaced with equal weight of sand and the system is ran to record corresponding noise, dynamic acceleration and dynamic force. The background measurements are subtracted from water filled case to get absolute values of noise, dynamic acceleration and dynamic force.

5.1.5 Consolidated Experimental Results

The complete parametric study is carried out as per table 5.1.

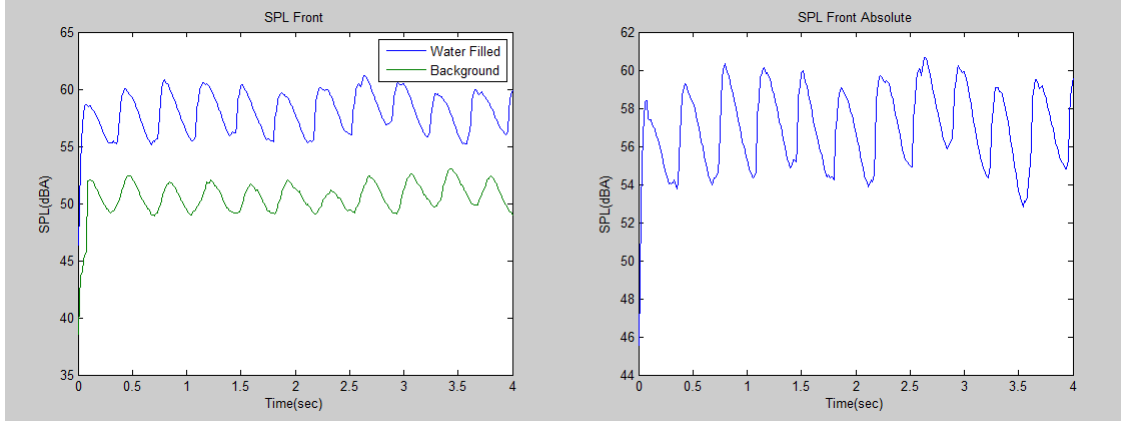


Figure 5.25: Background noise radiated from tank

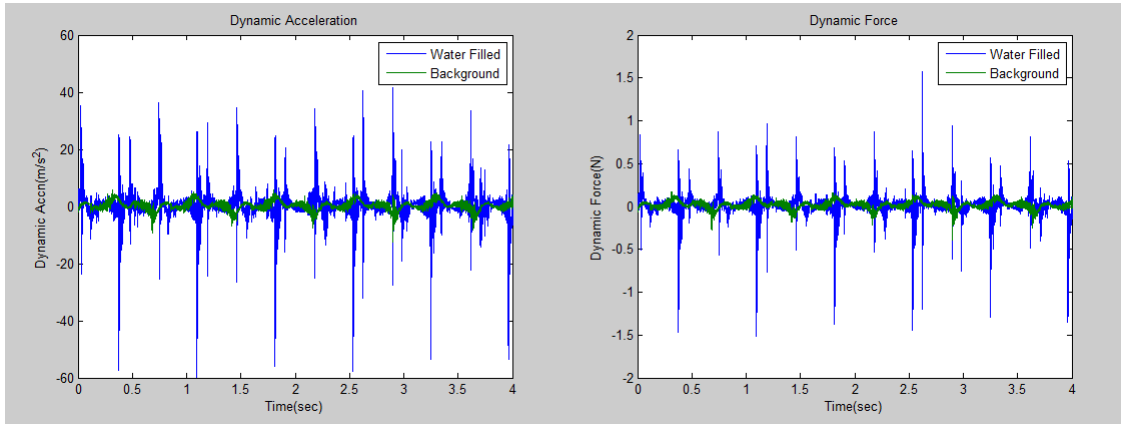


Figure 5.26: Background acceleration and force for tank

Peak noise, dynamic acceleration and dynamic force is recorded for each case after background measurement subtraction and averaging over the total number of cycles.

Figure 5.27 shows the variation of dynamic acceleration with excitation frequency for a particular fill level. It is clearly seen from the graph that the major dynamic activities occur when the external excitation frequency nears the sloshing natural frequency. This is the zone of nonlinear sloshing. Thus, the zone where the excitation frequency is close to sloshing natural frequency is important from sloshing noise point of view. The measured values are in agreement with the force calculated analytically by eqn 5.4:

$$F_w = m_f X_0 \Omega^2 \sin \Omega t \left\{ 1 + \sum_{n=0}^{\infty} \left[\frac{8 \tanh \left((2n+1) \frac{\pi h}{L} \right) \Omega^2}{(h/L) \pi^3 (2n+1)^3 (\omega_n^2 - \Omega^2)} \right] \right\} \quad (5.4)$$

The force obtained above is divided by m_f i.e. total mass of fluid to get acceleration. At resonance with sloshing natural frequency the analytical force tends to infinity, but at regions $0.7 * f_s$ to $0.9 * f_s$ can be used to predict the force analytically.

A waterfall graph is plotted with excitation frequency on X-axis, experimental dynamic

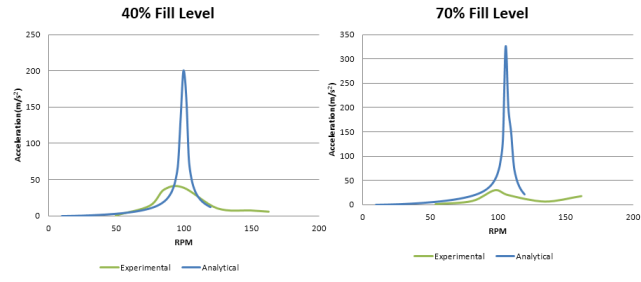


Figure 5.27: Variation of dynamic acceleration with excitation frequency

acceleration on Y-axis and percentage fill level as Z-axis. The graph is plotted for front, back and top wall.

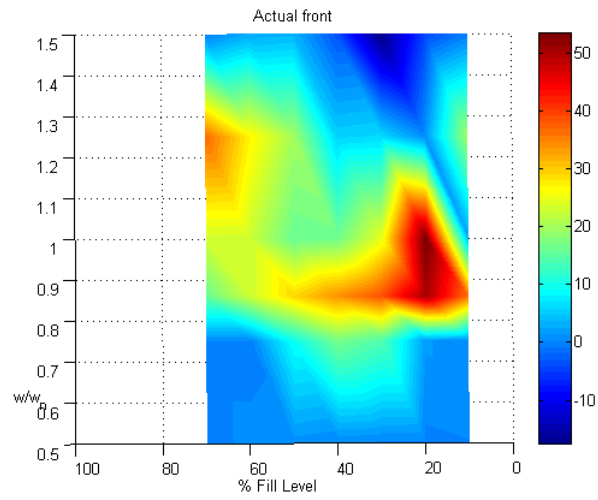


Figure 5.28: Waterfall graph of dynamic acceleration of front wall

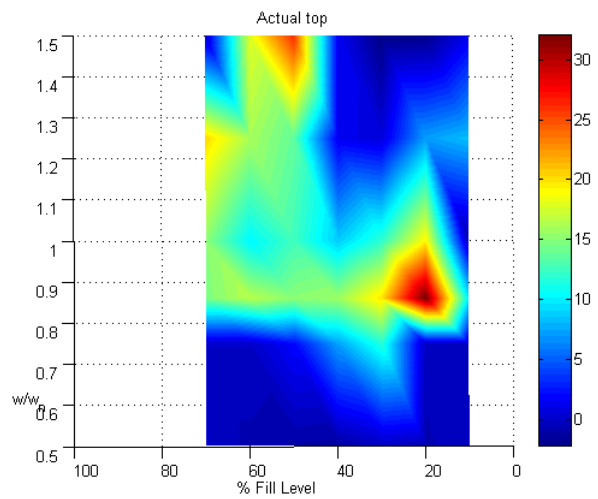


Figure 5.30: Waterfall graph of dynamic acceleration of top wall

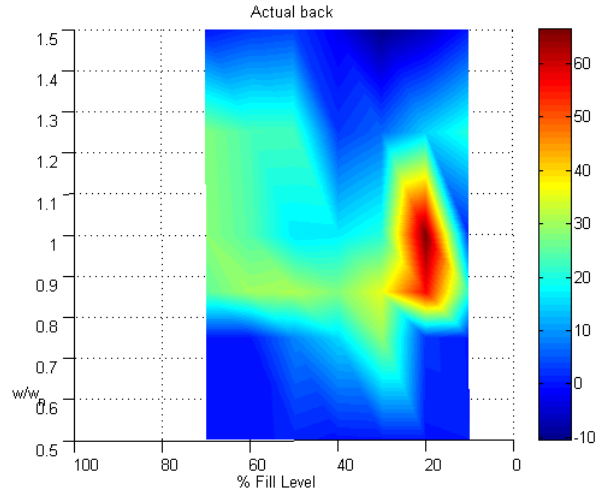


Figure 5.29: Waterfall graph of dynamic acceleration of back wall

It can be clearly observed that maximum dynamic forces, structure response and consequently noise radiation for front and back walls of tank occurs at lower fill levels(20% to 40%) and excitation frequency of $0.8*f_s$ to $1.2*f_s$ and hitting noise is predominant.

Also, maximum dynamic forces, structure response and consequently noise radiation for top wall of tank occurs at higher fill levels(40% to 70%) and excitation frequency of $0.8*f_s$ to $1.5*f_s$ and splashing noise is more dominant. The above mentioned zones are important from sloshing noise point of view as maximum noise is generated in these zones. The numerical methodology is validated in these zones.

5.1.6 Numerical Results

Sloshing hitting noise is dominant in regions when the external excitation frequency is near the sloshing natural frequency i.e. $1 f_s$. Numerical simulations are carried out in this zone i.e. 20% fill $1 f_s$, 40% fill $1 f_s$ and 60% fill $1 f_s$.

20% Fill $1 f_s$

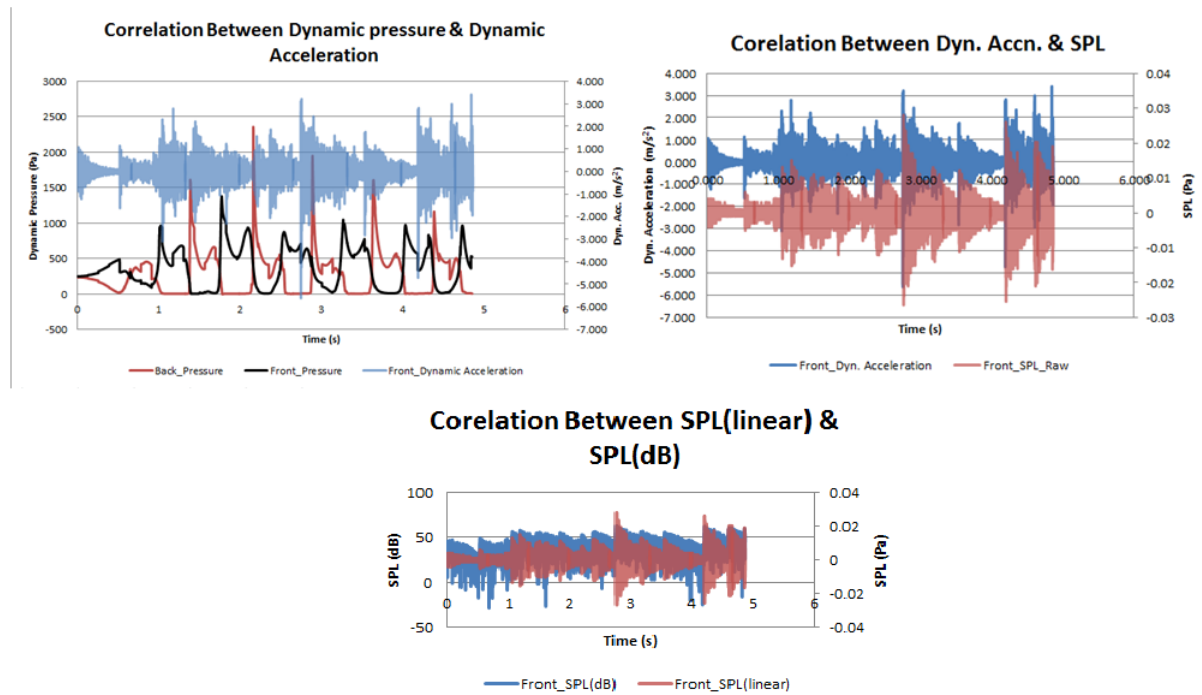


Figure 5.31: Correlation between Dynamic events

From figure 5.31 it is observed that dynamic pressure and dynamic acceleration of tank walls is synchronous; which suggests that when the fluid hits the tank walls vibrations are observed. Also dynamic acceleration and SPL is synchronous so that noise is generated due to these tank wall vibrations. These correlations between dynamic activities is also observed in experimental results.

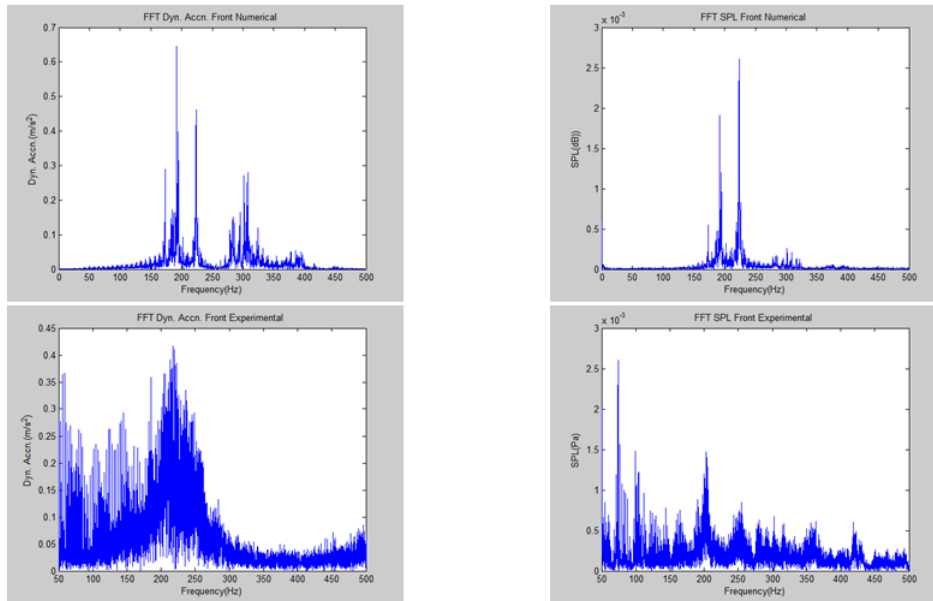


Figure 5.32: FFT Analysis for front dynamic acceleration and SPL

Figure 5.32 shows the FFT data for experimental and numerical dynamic acceleration and SPL. It is seen from the plot that experimental and numerical frequencies of dynamic acceleration and SPL is in close agreement. The frequency observed is 200 Hz which is close to the natural frequency of the tank with 20% fill level.

40% Fill $1 f_s$

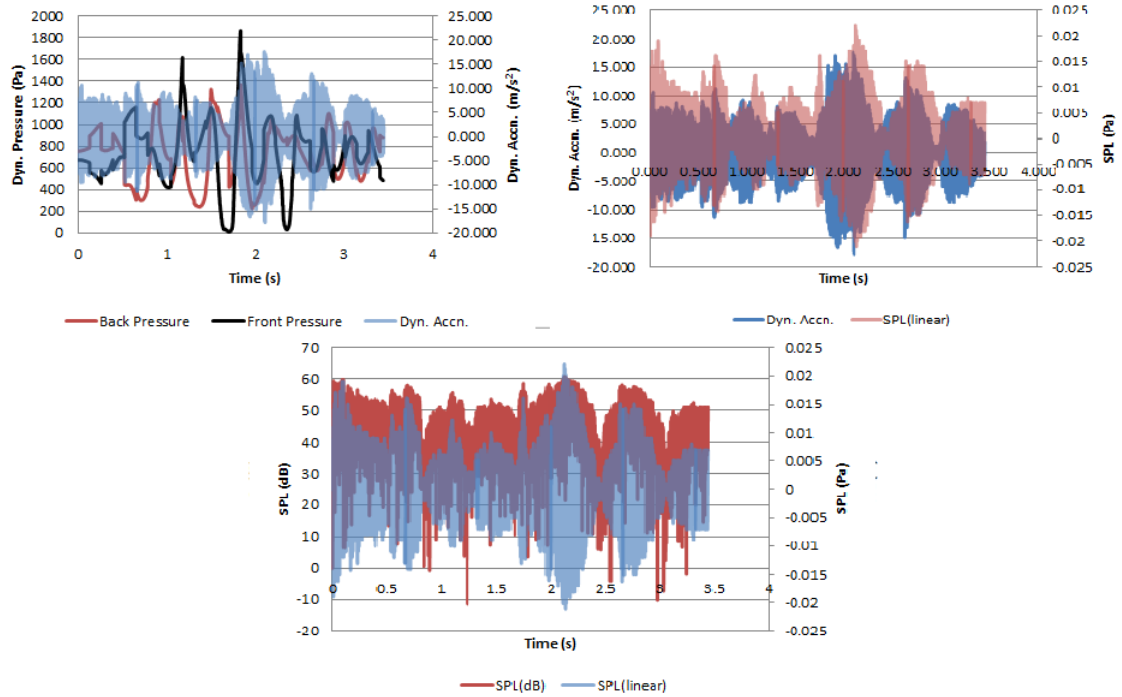


Figure 5.33: Correlation between Dynamic events

From figure 5.33 it is observed that dynamic pressure and dynamic acceleration of tank walls is synchronous; which suggests that when the fluid hits the tank walls vibrations are observed. Also dynamic acceleration and SPL is synchronous so that noise is generated due to these tank wall vibrations. These correlations between dynamic activities is also observed in experimental results.

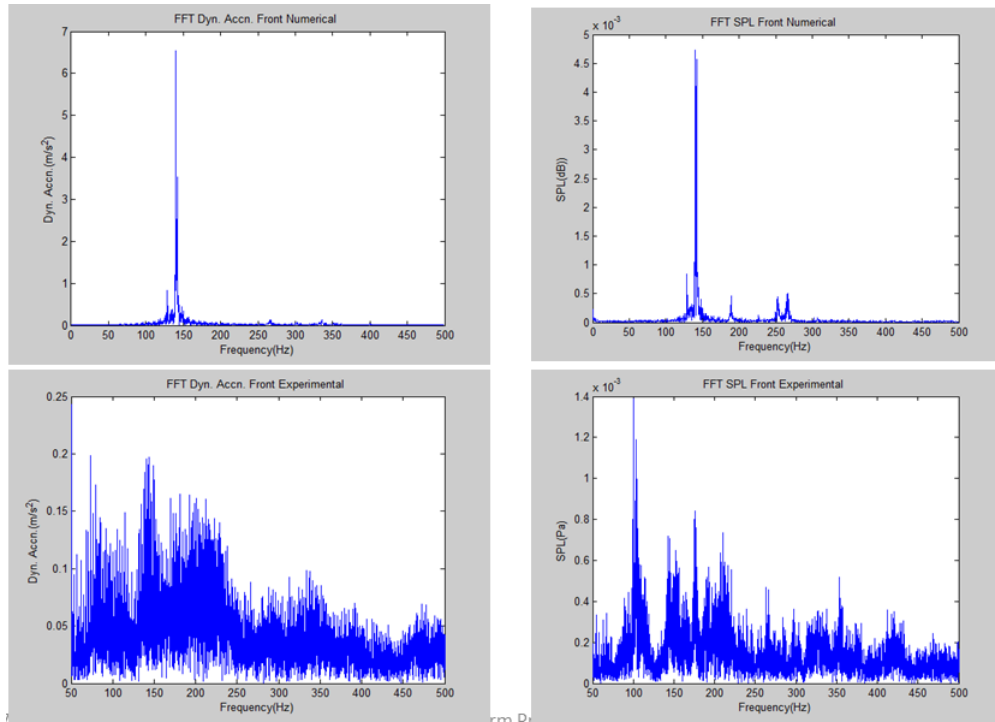


Figure 5.34: FFT Analysis for front dynamic acceleration and SPL

Figure 5.34 shows the FFT data for experimental and numerical dynamic acceleration and SPL. It is seen from the plot that experimental and numerical results of dynamic acceleration and SPL is in close agreement in frequency estimation. The frequency observed is 142 Hz which is close to the natural frequency of the tank with 40% fill level.

60% Fill $1 f_s$

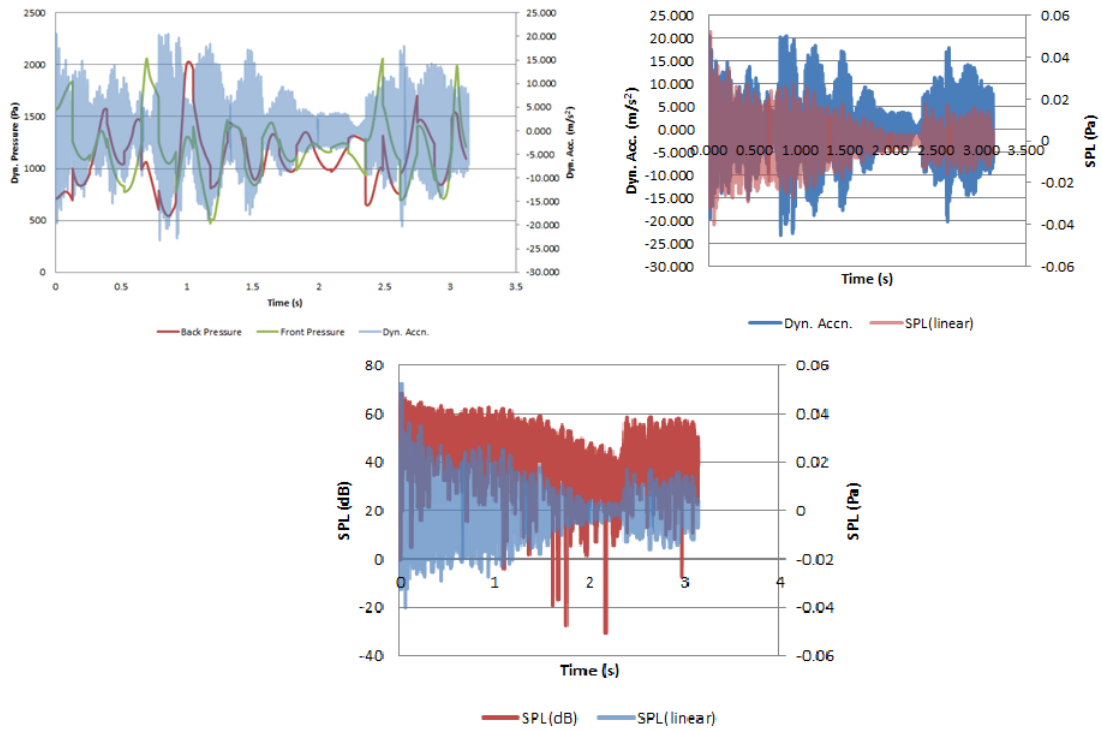


Figure 5.35: Correlation between Dynamic events

From figure 5.35 it is observed that dynamic pressure and dynamic acceleration of tank walls is synchronous; which suggests that when the fluid hits the tank walls vibrations are observed. Also dynamic acceleration and SPL is synchronous so that noise is generated due to these tank wall vibrations. These correlations between dynamic activities is also observed in experimental results.

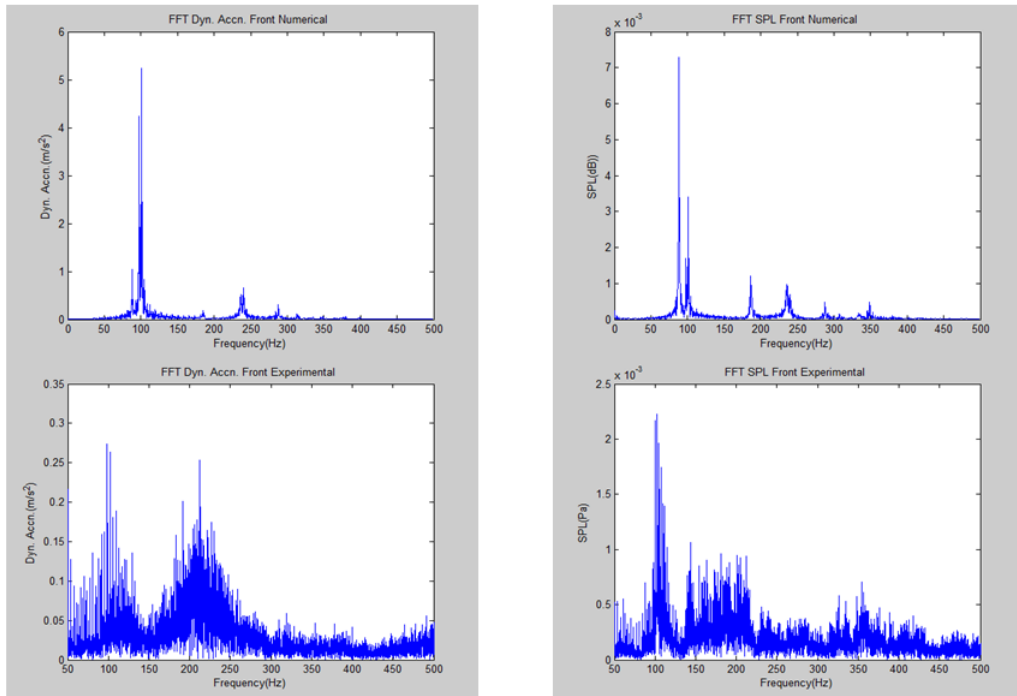


Figure 5.36: FFT Analysis for front dynamic acceleration and SPL

Figure 5.36 shows the FFT data for experimental and numerical dynamic acceleration and SPL. It is seen from the plot that experimental and numerical results of dynamic acceleration and SPL is in close agreement in frequency estimation. The frequency observed is 104 Hz which is close to the natural frequency of the tank with 60% fill level.

5.1.7 Comparison between Experimental and Numerical SPL

The peak SPL is compared for top and front microphones.

Table 5.4: Comparison of experimental and numerical results of SPL at Front Microphone position

% Fill	SPL(dB) Experimental	SPL(dB) Numerical	% Deviation
20% 1fs	60.8	61.4	-0.98684
40% 1fs	58	62.4	-7.58621
60% 1fs	58.1	61.4	-5.67986

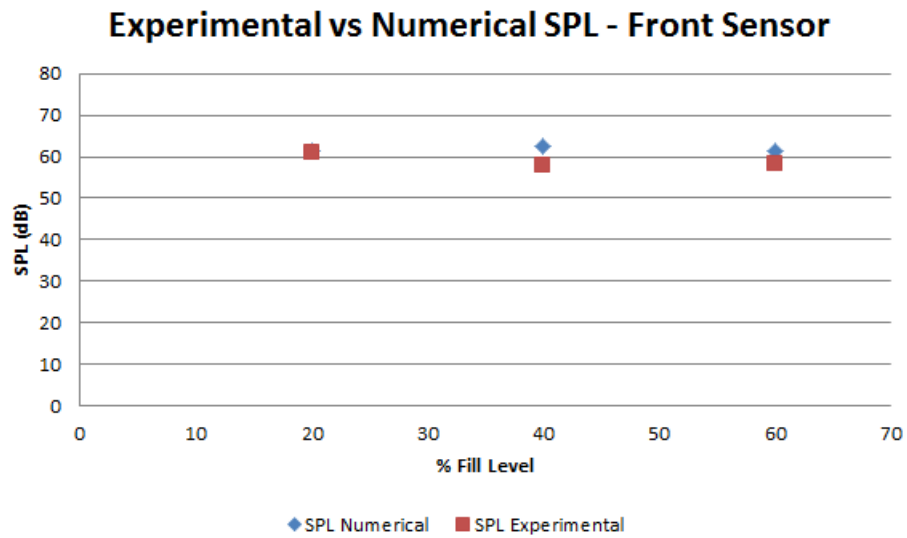


Figure 5.37: Comparison of experimental and numerical results of SPL at Front Microphone position

Table 5.5: Comparison of experimental and numerical results of SPL at Top Microphone position

% Fill	SPL(dB) Experimental	SPL(dB) Numerical	% Deviation
20% 1fs	62.15	59.7	3.942076
40% 1fs	57	64.3	-12.807
60% 1fs	59.4	60.6	-2.0202

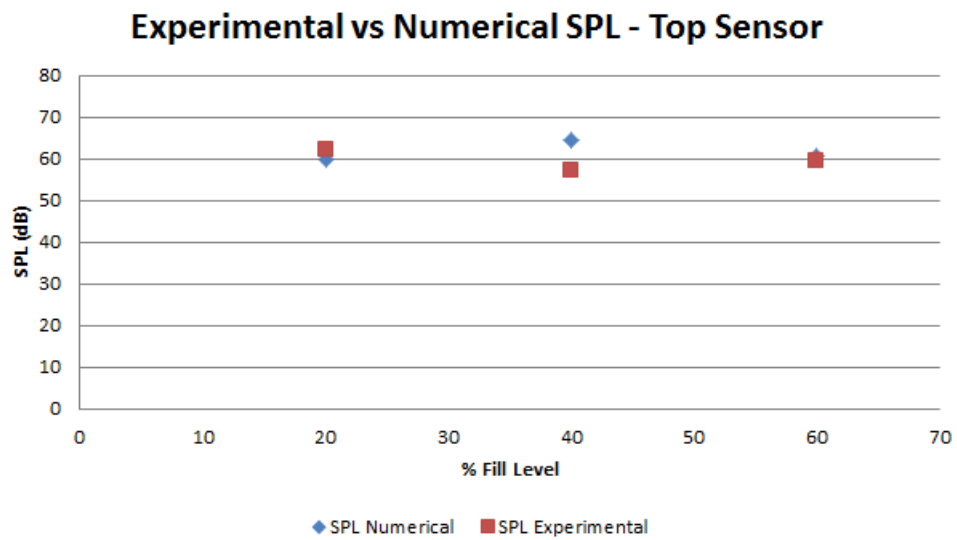


Figure 5.38: Comparison of experimental and numerical results of SPL at Top Microphone position

The results show that the numerical prediction results are able to estimate the trend of sloshing noise in the non linear zone.

Chapter 6

Summary and Future Scope

6.1 Summary

Experimental test setup has been developed to measure liquid sloshing noise under controlled excitation. Maximum dynamic activities occur when excitation frequency nears sloshing natural frequency. Sloshing natural frequency and dynamic forces on tank wall can be well predicted analytically in linear and weakly nonlinear regime. Parametric studies show that noise generation from front and back wall is dominant at fill levels lower than 40% and excitation frequency of $0.8*f_s$ to $1.2*f_s$ which is hitting noise. For top wall noise generation is dominant at fill levels higher than 40% and excitation frequency of $0.8*f_s$ to $1.5*f_s$ which is splashing noise. The experimental excitation can be controlled to get different zones of sloshing i.e. 1 fs for pure hitting and 2 fs for pure splashing. Fluid fill level has an effect on tank natural frequency i.e. natural frequency reduces with increasing fill level which is mainly due to mass loading effect of fluid on tank structure and thus fluid fill level has an effect on dynamic behaviour of tank. Numerical dynamic pressure, dynamic acceleration and SPL results are synchronous similar to experimental results. The numerical methodology well predicts sloshing noise.

6.2 Future Scope

1. Propose efficient computational methodology (active time duration, approximate dynamic force and location)
2. Simplified analytical model for noise prediction.
3. Extend the current methodology to actual fuel tank.

References

- [1] V. Jadon, G. Agawane, A. Baghel, V. Balide, R. Banerjee, A. Getta, H. Viswanathan, and A. Awasthi. An Experimental and Multiphysics Based Numerical Study to Predict Automotive Fuel Tank Sloshing Noise. Technical Report, SAE Technical Paper 2014.
- [2] C. Wachowski, J. Biermann, and R. Schala. Approaches to analyse and predict slosh noise of vehicle fuel tanks. In 24th International Conference of Noise and Vibration Engineering (ISMA2010), Belgium. 2010 .
- [3] M. Kamei, J. Hanai, W. Fukasawa, and T. Makino. Establishment of a method for predicting and confirming fuel tank sloshing noise. Technical Report, SAE Technical Paper 2007.
- [4] K. Kamiya, Y. Yamaguchi, and E. De Vries. Simulation Studies of Sloshing in a Fuel Tank. *Studies* 2011, (2002) 05–05.
- [5] P. De Man and J.-J. Van Schaftingen. Prediction of Vehicle Fuel Tank Slosh Noise from Component-Level Test Data. Technical Report, SAE Technical Paper 2012.
- [6] S. aus der Wiesche. Noise due to sloshing within automotive fuel tanks. *Forschung im Ingenieurwesen* 70, (2005) 13–24.
- [7] J.-S. Park, S.-C. Choi, and S.-G. Hong. The prediction of fuel sloshing noise based on fluid-structure interaction analysis. *SAE International Journal of Passenger Cars-Mechanical Systems* 4, (2011) 1304–1310.
- [8] V. V. S. Vytla and Y. Ando. Fluid Structure Interaction Simulation of Fuel Tank Sloshing. Technical Report, SAE Technical Paper 2013.
- [9] L. Khezzar, A. Seibi, and A. Goharzadeh. Water Sloshing in Rectangular Tanks—An Experimental Investigation & Numerical Simulation. *Int. J. of Engineering (IJE)* 3, (2009) 174–184.
- [10] M. Hattori, A. Arami, and T. Yui. Wave impact pressure on vertical walls under breaking waves of various types. *Coastal Engineering* 22, (1994) 79–114.

- [11] K. Thiagarajan, D. Rakshit, and N. Repalle. The air–water sloshing problem: Fundamental analysis and parametric studies on excitation and fill levels. *Ocean Engineering* 38, (2011) 498–508.
- [12] L. Hou, F. Li, and C. Wu. A numerical study of liquid sloshing in a two-dimensional tank under external excitations. *Journal of Marine Science and Application* 11, (2012) 305–310.
- [13] M. Peric and T. Zorn. Simulation of sloshing loads on moving tanks. In ASME 2005 24th International Conference on Offshore Mechanics and Arctic Engineering. American Society of Mechanical Engineers, 2005 1017–1026.
- [14] O. Jaiswal, S. Kulkarni, and P. Pathak. A study on sloshing frequencies of fluid-tank system. In Proceedings of the 14th World Conference on Earthquake Engineering. 2008 12–17.
- [15] H. S. Iu, W. Cleghorn, and J. Mills. Design and analysis of fuel tank baffles to reduce the noise generated from fuel sloshing. Technical Report, SAE Technical Paper 2004.
- [16] F. Li, S. D. Sibal, I. F. McGann, and R. Hallez. Radiated Fuel Tank Slosh Noise Simulation. Technical Report, SAE Technical Paper 2011.
- [17] G. J. DeSalvo and J. A. Swanson. ANSYS user’s manual. *Swanson Analysis Systems* .
- [18] S. U. Manual. LMS International. *Leuven, Belgium* .
- [19] D. A. Bies and C. H. Hansen. Engineering noise control: theory and practice. CRC Press, 2009.
- [20] S. Fraunhofer. MpCCI: Multidisciplinary Simulations through Code Coupling, Version 3.0. *MpCCI Manuals* .
- [21] F.-K. Benra, H. J. Dohmen, J. Pei, S. Schuster, and B. Wan. A Comparison of One-Way and Two-Way Coupling Methods for Numerical Analysis of Fluid-Structure Interactions. *Journal of applied mathematics* 2011.
- [22] R. A. Ibrahim. Liquid sloshing dynamics: theory and applications. Cambridge University Press, 2005.